



RESEARCH

Predefined-time adaptive consensus control for nonlinear multi-agent systems with input quantization and actuator faults

Li-Ting Lu · Shan-Liang Zhu · Dong-Mei Wang · Yu-Qun Han

Received: 21 March 2024 / Accepted: 28 May 2024 / Published online: 7 June 2024
© The Author(s), under exclusive licence to Springer Nature B.V. 2024

Abstract Predefined-time control has experienced substantial advancements in recent years. Nevertheless, the current technology has not achieved widespread adoption in nonlinear multi-agent systems (NMASs), and significant issues pertaining to the input quantization and actuator failures remain unaddressed. This paper investigates the problem of predefined-time consensus control for NMASs with input quantization and actuator faults. Notably, the study takes into account scenarios where each actuator may experience an infinite number of faults. In conjunction with practical predefined-time stability theory, an innovative predefined-time adaptive consensus control method has been developed within the framework of the backstepping method, incorporating the approximation technique of the multi-dimensional Taylor network (MTN). Additionally, by utilizing the characteristics of quantized nonlinear sectors and the structural model of actuator faults, novel adaptive estimation techniques are devised to handle the effects caused by actuator faults and quantized inputs. To further alleviate computational burdens and tackle the issue of computational explosion, a finite-time differentiator is employed to estimate the derivative of the virtual control. The pro-

posed control scheme achieves the desired performance of predefined-time convergence. Rigorous theoretical analyses indicate that the proposed control scheme can drive consensus errors to converge within a small range within a predefined-time, and users have the flexibility to choose the settling time. Moreover, all signals in the closed-loop system remain bounded. Finally, simulation results are provided to validate the effectiveness of the proposed approach.

Keywords Actuator faults · Predefined-time consensus control · Input quantization · Multi-dimensional Taylor network · Nonlinear multi-agent systems

1 Introduction

In recent years, cooperative control of multi-agent systems (MASs) has garnered significant attention [1–4] due to its ability to achieve complex objectives at a lower cost. The leader-follower consensus problem, one of the most important issues in cooperative control, has attracted significant interest. The core idea is to design controllers that utilize information from neighboring agents to enable all agents to track the trajectory of a leader. Notable progress has been made in addressing the leader-follower consensus problem in first-order [5], second-order [6], and high-order [7,8] MASs. However, the dynamic models in these research findings only involved simple unknown parameters or known nonlinear functions. As a result, when deal-

L.-T. Lu · S.-L. Zhu · D.-M. Wang · Y.-Q. Han
School of Mathematics and Physics, Qingdao University of Science and Technology, Qingdao 266061, China

S.-L. Zhu · Y.-Q. Han (✉)
Qingdao Innovation Center of Artificial Intelligence Ocean Technology, Qingdao 266061, China
e-mail: yuqunhan@qust.edu.cn

ing with systems characterized by intricate nonlinear behavior, these methods become ineffective. To address this challenge, an approximation-based intelligent control approach has been emerged. Noteworthy examples include fuzzy control [9–11], neural network control [12–14], and multi-dimensional Taylor network (MTN) control [15–19]. Although these methods offer rigorous stability proofs, they still possess some limitations. Firstly, the consensus time, a critical performance metric for the consensus tracking problem, has only been addressed in [10, 11]. Secondly, the authors in [10, 11] neglected the impact of quantization errors in control signals and assumed an infinite resolution for quantization, which is somewhat unrealistic. Additionally, they overlooked the possibility of actuator faults, which can greatly degrade the system's performance when they occur. Lastly, although MTN, as a novel approximation technique, offers advantages such as simplicity and low computational complexity, the previous researches on MTN control [15–19] have not been extended to NMASs. Therefore, this paper aims to design an MTN-based adaptive predefined-time consensus scheme for uncertain NMASs with actuator faults and input quantization, which is an open and meaningful problem.

On the one hand, while finite-time control method [20, 21] has been extensively researched over the years due to its rapid convergence speed and robustness against complex disturbances, the convergence time of finite-time control is subject to the initial conditions, which can be challenging to precisely determine in practical systems [22]. To address this limitation, fixed-time control was proposed in [22], offering the advantage of ensuring system convergence within a finite time while guaranteeing an upper bound on the convergence time solely determined by design parameters, independent of initial conditions. Consequently, fixed-time control has found application in systems with convergence time requirements, such as power system control [23] and teleoperation system control [24]. However, the intricate relationship between the design parameters and the settling time bound in fixed-time control poses challenges in establishing a direct correlation between them, making it difficult to design and adjust parameters to meet desired convergence time requirements. To further improve the performance of fixed-time control, the concept of predefined-time control was introduced in [25]. Unlike fixed-time control, the convergence time of a predefined time stable system

explicitly appears in parameter tuning. This means that it is possible to arbitrarily specify the desired convergence time, and the design parameters of the controller can be determined based on this specified convergence time. In recent times, predefined-time control has been extended to various types of nonlinear systems, such as general nonlinear systems [26, 27], stochastic nonlinear systems [28], and switched nonlinear systems [29]. It is noteworthy that while predefined-time control aids in control protocol gains and reducing conservative limits on estimated consensus time in leader-follower consensus, research on predefined-time control in leader-follower consensus remains relatively limited.

On the other hand, in practical industrial applications, two challenges arise when the designed control signal is transmitted from the actuator to the actual system: signal quantization and actuator faults. Various systems, such as discrete nonlinear stochastic systems [30], hybrid systems [31], and networked systems [32], inherently involve quantized signals. Therefore, considering quantizers in control system design becomes highly relevant as they effectively convert continuous control signals into feasible quantized signals, thereby reducing the burden of signal communication. Significant advancements [33–35] have been made in the field of quantized control over the past two decades. The authors in [34] proposed a linear decomposition based on hysteresis quantizers, but it imposed significant restrictions on the system due to the inability of the perturbation terms to guarantee the constraints of control-independent constants. Subsequently, a novel decomposition method based on hysteresis quantizers was introduced in [35], effectively addressing the limitations of the previous approach. Despite its benefits, this new decomposition introduces dynamic control coefficients that pose challenges in controller design, particularly when each actuator of the system may repeatedly encounter failures. The authors in [36] successfully tackled the potential for infinite occurrences of failures in each actuator of the system by employing a boundary estimation approach to design the controller. Inspired by their work, the authors in [37] tackled the formidable task of handling the significant nonlinearity introduced by quantization decomposition and actuator faults by estimating the bounds of time-varying effectiveness factors for quantizer parameters and actuator fault parameters. This approach successfully addressed a significant gap in current research. However, it's crucial to emphasize that applying this

approach to NMASs while accommodating predefined consensus time presents a formidable challenge. This challenge stems from substantial obstacles in analyzing the stability of predefined-time, exacerbated by actuator failures and input quantization. As a result, attaining leader-follower consensus control within predefined timeframes in NMASs holds significant importance. However, advancements in extending this method to NMASs encountering actuator failures and input quantization have been somewhat constrained due to the complex challenges involved in mathematical analysis.

Inspired by the above discussion, while the issue of predefined-time adaptive consensus control for NMASs with input quantization and actuator faults is crucial, it has not received significant attention in current literature. Therefore, addressing this problem constitutes a meaningful research topic. The aim of this study is to bridge this research gap by employing backstepping techniques. The primary contributions can be summarized as follows

- (1) The paper presents, for the first time, an adaptive predefined-time consensus control scheme based on MTN for NMASs with input quantization and actuator faults. Unlike existing approaches in adaptive fuzzy control [9–11] and neural network control [12–14] that only tackle either actuator faults, input quantization, or predefined-time issues individually, the scenarios addressed in this paper are more comprehensive and have a wider application scope. Simultaneously, despite the advantages of MTN such as reduced computational complexity and fast approximation, previous research on MTN control [15–19] had not explored its application in NMASs. This paper represents the first instance of applying MTN control to NMASs, signifying a significant and important extension in this context.
- (2) Compared to existing finite-time and fixed-time control schemes in [20, 21, 23, 24], the most compelling aspect of this proposed method is its ability to predefine the required settling time, which users can freely select irrespective of the system's initial conditions. Despite the capability of the prescribed time control scheme [38, 39] to arbitrarily design a settling time, it frequently necessitates the definition of a scalar function. This not only introduces significant complexity to the controller's construction but also poses challenges in parameter selection.
- (3) In this paper, the controller is constructed based on the theory of predefined-time stability. The consensus gain is intricately connected to the consensus time, simplifying the determination of control protocol gains and thereby broadening its applicability.
- (3) Compared to the scenarios discussed in [10, 11], this research extends its scope to include the presence of quantized inputs and actuator faults, which are commonly encountered in most practical systems. In order to address these characteristics simultaneously, this study proposes a novel estimation method for the upper bounds of quantization parameters and actuator fault parameters. Furthermore, the constructed controller is capable of handling an infinite number of failures occurring in each actuator, making it highly practical for practise engineering models.

2 Problem formulations and preliminaries

2.1 Graph theory

The communication topology of NMASs can be represented as a directed graph $\zeta = (\mathcal{V}, \mathcal{C}, \mathcal{A})$, where $\mathcal{V} = \{1, 2, \dots, N\}$ represents the set of nodes, $\mathcal{C} \subseteq \mathcal{V} \times \mathcal{V}$ represents the set of edges, and $\mathcal{A} = [a_{i,k}] \in \mathbb{R}^{N \times N}$ is the adjacency matrix that captures the communication relationships between nodes. If node i can receive messages from node k , it is defined as $a_{i,k} = 1$; otherwise, $a_{i,k} = 0$. It is also assumed that $a_{i,i} = 0$. In this context, if node i can receive messages from node k , node k is referred to as a neighbor of node i . The set of neighboring nodes of agent i is defined as $\mathcal{N}_i = \{\mathcal{V}_k | (\mathcal{V}_k, \mathcal{V}_i) \in \mathcal{C}, i \neq k\}$. The degree of node i is defined as $d_i = \sum_{k \in \mathcal{N}_i} a_{i,k}$, and the Laplacian matrix of the directed graph is given by $\mathcal{L} = \mathcal{D} - \mathcal{A}$, where $\mathcal{D} = \text{diag}\{d_i\}$. If the leader agent 0 is involved, the enhanced graph $\bar{\zeta} = (\bar{\mathcal{V}}, \bar{\mathcal{C}})$ is obtained, where $\bar{\mathcal{V}} = \mathcal{V} \cup \{0\}$ and $\bar{\mathcal{C}} \subseteq \bar{\mathcal{V}} \times \bar{\mathcal{V}}$. The connectivity matrix between followers and the leader can be represented as $\mathcal{B} = \text{diag}\{r_i\}$, where $r_i = 1$ indicates that the agent i can receive information from the leader, and $r_i = 0$ otherwise.

2.2 Problem formulation

Consider the following NMASs with input quantization and actuator faults

$$\begin{cases} \dot{x}_{i,j} = \phi_{i,j}(\bar{x}_{i,j})x_{i,j+1} + \sigma_{i,j}(\bar{x}_{i,j}) + d_{i,j}(t) \\ \dot{x}_{i,n} = \sum_{l=1}^{m_i} \phi_{i,nl}(\bar{x}_{i,n})q^f(u_{i,l}) + \sigma_{i,n}(\bar{x}_{i,n}) + d_{i,n}(t) \\ y_i = x_{i,1}, i = 1, 2, \dots, N, j = 1, 2, \dots, n - 1 \end{cases} \quad (1)$$

where $\bar{x}_{i,j} = [x_{i,1}, x_{i,2}, \dots, x_{i,j}]^T \in R^j$ represents the state vector of the followers, while $y_i \in R$ denotes the output of the i -th follower. $\phi_{i,j}(\bar{x}_{i,j}) : R^j \rightarrow R$ and $\phi_{i,nl}(\bar{x}_{i,n}) : R^n \rightarrow R$ represent control gains with know signs. $\sigma_{i,j}(\bar{x}_{i,j})$ are uncertain continuous functions, and $d_{i,j}(t)$ represents time-varying disturbances and there exists a positive value $\bar{d}_{i,j}$ that satisfies $|d_{i,j}| \leq \bar{d}_{i,j}$. $q^f(u_{i,l})$ denotes the quantized input signals that are influenced by actuator faults, with $u_{i,l}$ representing the control input signals.

Remark 1 In practical applications, numerous physical phenomena adhere to the dynamics described by system (1), encompassing scenarios like the movement of aircraft wings [40], the operation of robotic manipulators [41], and the control of ship steering systems [42]. Furthermore, the specific challenge of implementing adaptive predefined-time consensus control for NMASs (1) with input quantization and actuator failures remains unresolved in current knowledge and research.

In this paper, the input model of the hysteresis quantizer is consistent with the model described in [12], which can be represented as follows

$$q(u_{i,l}) = \begin{cases} u_{i,lc} \operatorname{sgn}(u_{i,l}), & \frac{u_{i,lc}}{1+\delta_{i,l}} \leq |u_{i,l}| \leq u_{i,lc}, \dot{u}_{i,l} < 0 \\ & \text{or } u_{i,lc} < |u_{i,l}| \leq \frac{u_{i,lc}}{1-\delta_{i,l}}, \\ & \dot{u}_{i,l} > 0 \\ u_{i,lc}(1 + \delta_{i,l}) \operatorname{sgn}(u_{i,l}), & u_{i,lc} < |u_{i,l}| \leq \frac{u_{i,lc}}{1-\delta_{i,l}}, \dot{u}_{i,l} < 0 \\ & \text{or } \frac{u_{i,lc}}{1-\delta_{i,l}} < |u_{i,l}| \leq \frac{u_{i,lc}(1+\delta_{i,l})}{1-\delta_{i,l}}, \\ & \dot{u}_{i,l} > 0 \\ 0, & 0 \leq |u_{i,l}| < \frac{u_{i,l\min}}{1+\delta_{i,l}}, \dot{u}_{i,l} < 0 \\ & \text{or } \frac{u_{i,l\min}}{1+\delta_{i,l}} \leq |u_{i,l}| < u_{i,l\min}, \\ & \dot{u}_{i,l} > 0 \\ q(u_{i,l}(t^-)), & u_{i,l} = 0 \end{cases} \quad (2)$$

where $u_{i,lc} = \rho_{i,l}^{1-c} u_{i,l\min}$, ($c = 1, 2, \dots$). Before quantizing the input signal at each sampling time, the

quantizer can compute a unique value of c . $u_{i,l\min} > 0$ represents the quantization dead-zone. When the signal is smaller than the dead-zone value, the quantized signal remains zero regardless of whether the input signal increases or decreases. $\delta_{i,l} = \frac{1-\rho_{i,l}}{1+\rho_{i,l}}$, where $0 < \rho_{i,l} < 1$ represents the step size of quantization density. In simpler terms, a higher value of $\delta_{i,l}$ indicates a coarser quantization of the signal, while a lower value corresponds to a finer quantization.

Remark 2 To alleviate the communication load within the network, it is essential to employ coarser quantizers for quantizing control signals with high rates of change. The parameter $\delta_{i,l}$, which lies within the range of $(0, 1)$, dictates the quantization level of the hysteresis quantizer. As $\delta_{i,l}$ increases, the quantization level decreases, resulting in a coarser quantization of the control signals. Therefore, an intriguing task is to achieve satisfactory control performance with fewer quantization levels. As demonstrated in the subsequent sections, by constructing a novel adaptive controller, the restrictive conditions imposed on the quantizer parameter $\delta_{i,l}$ and system uncertainties in [34] are eliminated.

However, in practical engineering scenarios, actuators are prone to failures. Inspired by [37], the failure of the l -th actuator in the i -th agent can be modeled as

$$q^f(u_{i,l}) = \varrho_{i,lh} q(u_{i,l}) + \bar{u}_{i,lh}, t \in [t_{lh,b}, t_{lh,e}] \quad (3)$$

$$\varrho_{i,lh} \bar{u}_{i,lh} = 0, i = 1, 2, \dots, N, l = 1, 2, \dots, m_i$$

where $h = 1, 2, 3, \dots$ represents the occurrence of failures, $\varrho_{i,lh} \in [0, 1]$ and $\bar{u}_{i,lh}$ denote unknown time-varying fault parameters. $t_{lh,b}$ and $t_{lh,e}$ represent the onset and end time of the h -th occurrence of a failure, respectively. It is important to note that the actuator fault model under consideration encompasses three distinct scenarios, each applicable to different situations

- (1) When $\varrho_{i,lh} = 1$ and $\bar{u}_{i,lh} = 0$, the actuator is functioning normally without any faults.
- (2) When $0 < \varrho_{i,lh} < 1$ and $\bar{u}_{i,lh} = 0$, the actuator has encountered partial loss of effectiveness failures.
- (3) When $\varrho_{i,lh} = 0$ and $\bar{u}_{i,lh} \neq 0$, the actuator has encountered total loss of effectiveness failures.

The control objective of this paper is to design a predefined-time consensus control scheme for NMASs (1) with input quantization and actuator faults. The controller aims to satisfy two crucial criteria: (1) ensuring that the output y_i of the agents achieves consensus with the given reference signal y_d within a predefined-time;

(2) guaranteeing the boundedness of all signals in the closed-loop system.

To accomplish the objectives, the following assumptions are necessary.

Assumption 1 The signal of the leader, denoted as y_d , and its derivatives up to the n -th order with respect to time are continuously bounded.

Assumption 2 The directed graph ζ has a spanning tree with the leader as its root node.

Assumption 3 In the case of partial failure, the fault parameter $q_{i,lh}(t)$ has an unknown constant $\underline{q}_{i,lh}$ such that $0 < \underline{q}_{i,lh} \leq q_{i,lh}(t) < 1$. In the case of stuck failure, the fault parameter $\bar{u}_{i,lh}(t)$ has an unknown constant $\bar{u}_{i,lh} > 0$ such that $|\bar{u}_{i,lh}(t)| \leq \bar{u}_{i,lh}$, where $i = 1, 2, \dots, N, l = 1, 2, \dots, m_i$.

Assumption 4 At any given time, at most $m_i - 1$ actuators can experience total loss of effectiveness failures.

Assumption 5 The signs of $\phi_{i,j}$ and $\phi_{i,nl}$ are positive, and there exist positive constants $\bar{\phi}_{i,j}, \underline{\phi}_{i,j}, \bar{\phi}_{i,nl}$, and $\underline{\phi}_{i,nl}$ such that $0 < \underline{\phi}_{i,j} \leq \phi_{i,j} \leq \bar{\phi}_{i,j}$ and $0 < \underline{\phi}_{i,nl} \leq \phi_{i,nl} \leq \bar{\phi}_{i,nl}$.

Remark 3 In practical engineering applications, the leader’s output y_d can be accurately characterized by both a differential equation and a bounded equation. Hence, its practicality is highly meaningful, and Assumption 1 is justified. Assumption 2 posits the existence of at least one follower agent capable of directly acquiring information from the leader, while the remaining agents can indirectly access the leader’s information through directed pathways. Assumptions 1 and 2 can both be found in [43,44]. Assumptions 3-5 constitute essential requirements for adaptive backstepping control and fault-tolerant control schemes, as evidenced in numerous studies [9,33,34,36]. Assumption 3 implies that the controller designed to compensate for an infinite number of faults only utilizes the boundary values of unknown parameters. Therefore, in the context of control engineering, this is reasonable. Assumption 4 is a fundamental condition for system controllability. As long as at least one actuator is not in a total loss of effectiveness state, simultaneous occurrence of partial loss of effectiveness or total loss of effectiveness state states in the actuators is allowed.

2.3 Preliminaries

This section will introduce some useful definitions and lemmas for control protocol development and stability analysis.

Definition 1 [45]: For a system $\dot{x} = f(x)$ with the origin as the equilibrium point, the equilibrium is considered to be practically predefined-time stable if there exist constants $\check{\gamma} > 0$ and $T > 0$ such that $\|x\| \leq \check{\gamma}$ holds for all $t > T$, where $x \in R^n$ represents the system state and $f : R^n \rightarrow R$ represents the nonlinear function. The parameter T is referred to as the predefined-time.

Remark 4 In traditional finite-time control, the settling time is generally influenced by the initial state. In fixed-time control, the boundary of settling time is associated with the controller parameters. It can be challenging task to adjust the parameters based on the desired settling time in finite/fixed-time control.

Lemma 1 [12]: If Assumption 2 holds, then $\mathcal{L} + \mathcal{B} > 0$, where \mathcal{L} and \mathcal{B} have already been defined in the previous graph theory.

Lemma 2 [26]: For the system $\dot{x} = f(x)$, if there exists a Lyapunov function V satisfying the following conditions

$$\dot{V} \leq -\frac{\pi}{\zeta T_s} \left(V^{1+\frac{\zeta}{2}} + V^{1-\frac{\zeta}{2}} \right) + \Gamma \tag{4}$$

where $0 < \zeta < 1, T_s > 0$, and $\Gamma > 0$ are constants, then the system $\dot{x} = f(x)$ is considered as practically predefined-time stable, and V can remain within the range $V \leq \frac{\zeta \Gamma T_s}{\pi}$ for a predefined-time of $2T_s$.

Lemma 3 [35]: The hysteresis quantizer $q(u_{i,l})$ can be decomposed into the following representation

$$q(u_{i,l}) = P(u_{i,l})u_{i,l} + R_{i,l} \tag{5}$$

where $P(u_{i,l})$ and $R_{i,l}$ fulfill the following conditions

$$1 - \delta_{i,l} \leq P(u_{i,l}) \leq 1 + \delta_{i,l}, |R_{i,l}| \leq u_{i,l} \min \tag{6}$$

Remark 5 Unlike the traditional linear decomposition $q(u(t)) = u(t) + d(t)$, where the perturbation term $d(t)$ needs to satisfy $|d(t)| \leq |\delta u(t)|$, making it challenging to explicitly define its bounds. This paper employs a novel nonlinear decomposition method proposed in [35]. This method effectively resolves the

difficulty in ensuring the boundedness of $d(t)$. Subsequently, conventional analysis tools like MTN control theory can be utilized to investigate the quantization effects. This approach effectively eliminates the restrictions imposed in [34] regarding the quantization parameters and uncertain functions. Nevertheless, it's important to highlight that, despite the incorporation of novel nonlinear decomposition techniques in this study, it presents considerable hurdles for controller design. These hurdles become particularly conspicuous in the face of actuator failures and the imperative for consensus on predefined-time, which the paper subsequently endeavors to tackle.

Lemma 4 [16]: For any continuous function $F(X)$ defined on a compact set Ω_x , there exists an MTN with a form of $H^T \Phi_{m_n}$ that can be used to approximate $F(X)$. The expression is as follows

$$F(X) = H^T \Phi_{m_n}(X) + \epsilon(X) \tag{7}$$

where $X = [x_1, x_2, \dots, x_n]^T \in \Omega_x$ indicates the input vector of MTN. $H = [h_1, h_2, \dots, h_p]^T \in R^p$ is the weight vector of MTN, $\Phi_{m_n}(X) = [x_1, \dots, x_n, x_1^2, x_1 x_2, \dots, x_n^2, x_1^m, x_1^{m-1} x_2, \dots, x_n^m]^T \in R^p$ means the middle layer vector of MTN. $\epsilon(X)$ represents the approximation error. And there exists a positive constant $\bar{\epsilon}$ such that $|\epsilon(X)| < \bar{\epsilon}$.

Lemma 5 [27]: Introduce the finite time differentiator as

$$\begin{cases} \dot{\chi}_1 = -\ell_1 \text{sig}(\chi_1 - \alpha(t)) + \chi_2 \\ \dot{\chi}_2 = -\ell_2 \text{sign}(\chi_2 - \alpha(t)) \end{cases} \tag{8}$$

where $\text{sig}(\chi_1 - \alpha(t)) = |\chi_1 - \alpha(t)|^{\frac{1}{2}} \text{sign}(\chi_1 - \alpha(t))$, χ_1, χ_2 represent the states of the differentiator; ℓ_1 and ℓ_2 represent the parameters of the differentiator. $\alpha(t)$ is unknown function. Furthermore, if the initial deviations $\chi_1(0) - \alpha(0)$ and $\chi_2(0) - \alpha(0)$ are bounded, the differentiator (8) can provide $\dot{\alpha}(t)$ with arbitrary accuracy. Additionally, it holds that $\dot{\alpha}(t) = \chi_2 + \varepsilon$, where there exists $\bar{\varepsilon} > 0$ such that ε satisfies $|\varepsilon| < \bar{\varepsilon}$.

Lemma 6 [46]: Consider the following differential equation

$$\dot{\hat{k}}(t) = -\check{c}\hat{k}(t) - \check{b}\hat{k}^s(t) + \check{d}v(t) \tag{9}$$

where $\check{c}, \check{b}, \check{d} > 0, s > 1$ are constants, and $v(t)$ represents a positive function. If $\hat{k}(0) \geq 0$, then $\hat{k}(t) \geq 0$ for $\forall t \geq 0$.

Lemma 7 [36]: For any positive bounded and uniform continuous function $\varpi(t)$ and any variable x , one has

$$0 \leq |x| - \frac{x^2}{\sqrt{x^2 + \varpi(t)^2}} < \varpi(t) \tag{10}$$

Lemma 8 [47]: For $x \in R, y \in R$ and positive constants $a_f > 0, b_f > 0, \delta_f > 0$, one has

$$\begin{aligned} |x|^{a_f} |y|^{b_f} &\leq \frac{a_f}{a_f + b_f} \delta_f |x|^{a_f + b_f} \\ &\quad + \frac{b_f}{a_f + b_f} \delta_f^{-\frac{a_f}{b_f}} |y|^{a_f + b_f} \end{aligned} \tag{11}$$

Lemma 9 [47]: For $y \geq x$, and $\aleph > 1$, one has

$$x(y - x)^\aleph \leq \frac{\aleph}{1 + \aleph} (y^{1+\aleph} - x^{1+\aleph}) \tag{12}$$

Lemma 10 [45]: For $x_i \in R, 0 < r_f < 1, \underline{r}_f \geq 1, i = 1, \dots, n$, one has

$$\begin{aligned} \left(\sum_{i=1}^n x_i \right)^{r_f} &\leq \sum_{i=1}^n x_i^{r_f}, \\ \left(\sum_{i=1}^n x_i \right)^{\underline{r}_f} &\leq n^{\underline{r}_f - 1} \left(\sum_{i=1}^n x_i^{\underline{r}_f} \right) \end{aligned} \tag{13}$$

Remark 6 Despite the need for the aforementioned ten lemmas in this paper, they do not introduce significant conservatism to its findings. This is because these lemmas serve more as facilitative tools for the paper. They not only provide theoretical foundations but also offer necessary support for subsequent derivations and analyses. Therefore, despite the relatively large number of lemmas, their primary function is to enhance the credibility and reliability of the research, rather than adding conservatism to it.

3 Predefined-time adaptive controller design

In this section, we propose an adaptive predefined-time control scheme based on the backstepping method. The MTN approach is employed throughout each step to approximate the unknown nonlinear functions. Additionally, we introduce an improved method for estimating unknown parameters, compensating for actuator faults and input quantization in the NMASs. To begin

with, the following transformations are introduced as

$$\begin{cases} e_{i,1} = \sum_{k=1}^N a_{i,k}(y_i - y_k) + r_i(y_i - y_d) \\ e_{i,j} = x_{i,j} - \alpha_{i,j-1}, i = 1, 2, \dots, N, j = 2, \dots, n \end{cases} \quad (14)$$

where $a_{i,k}$ represents the weight between the i -th agent and the k -th agent, r_i denotes the gain between the leader and the followers, y_d represents the leader's signal and $\alpha_{i,j-1}$ represents the virtual control signals. Define a constant $\mu_i = \max \{ \|H_{i,j}\|^2, j = 1, 2, \dots, n \}$, where $H_{i,j}$ represents the weight vector of the MTN. Then, let $\tilde{\mu}_i = \mu_i - \hat{\mu}_i$, where $\hat{\mu}_i$ is the estimation of μ_i . Based on the proposed control scheme, the virtual and actual controllers are constructed as follows

$$\alpha_{i,j} = -\frac{1}{\phi_{i,j}^{l_i}} \frac{e_{i,j} \check{\alpha}_{i,j}^2}{\sqrt{e_{i,j}^2 \check{\alpha}_{i,j}^2 + \varpi_i^2}}, \quad j = 1, 2, \dots, n - 1 \quad (15)$$

$$u_{i,l} = -\frac{1}{(1 - \delta_{i,l})} \frac{e_{i,n} \hat{\lambda}_i^2 \check{\alpha}_{i,n}^2}{\sqrt{e_{i,n}^2 \hat{\lambda}_i^2 \check{\alpha}_{i,n}^2 + \varpi_i^2}}, \quad l = 1, 2, \dots, m_i \quad (16)$$

where if $j = 1, l_i = A_i$, otherwise $l_i = 1$. The intermediate virtual control signals, denoted by $\check{\alpha}_{i,j}$, are defined as follows

$$\begin{aligned} \check{\alpha}_{i,1} &= \frac{1}{2}^{1+\frac{\zeta}{2}} c_{i,1} M_{i,1}(e_{i,1}) + \frac{1}{2}^{1-\frac{\zeta}{2}} c_{i,2} N_{i,1}(e_{i,1}) \\ &+ \frac{\hat{\mu}_i e_{i,1} \Phi_{m_{i,1}}^T \Phi_{m_{i,1}}}{2\check{\alpha}_{i,1}^2} \\ &+ \frac{1 + A_i + \sum_{k=1}^N a_{i,k}}{2} e_{i,1} \end{aligned} \quad (17)$$

$$\begin{aligned} \check{\alpha}_{i,j} &= \frac{1}{2}^{1+\frac{\zeta}{2}} c_{i,1} M_{i,j}(e_{i,j}) + \frac{1}{2}^{1-\frac{\zeta}{2}} c_{i,2} N_{i,j}(e_{i,j}) \\ &+ \frac{\hat{\mu}_i e_{i,j} \Phi_{m_{i,j}}^T \Phi_{m_{i,j}}}{2\check{\alpha}_{i,j}^2} \\ &+ e_{i,j} + \text{sign}(e_{i,j})(\bar{\epsilon}_{i,j-1} \\ &+ J_i \bar{\phi}_{i,j-1} |e_{i,j-1}|) - \chi_{i,(j-1)2}, \\ &j = 2, 3, \dots, n - 1 \end{aligned} \quad (18)$$

$$\begin{aligned} \check{\alpha}_{i,n} &= \frac{1}{2}^{1+\frac{\zeta}{2}} c_{i,1} M_{i,n}(e_{i,n}) + \frac{1}{2}^{1-\frac{\zeta}{2}} c_{i,2} N_{i,n}(e_{i,n}) \\ &+ \frac{\hat{\mu}_i e_{i,n} \Phi_{m_{i,n}}^T \Phi_{m_{i,n}}}{2\check{\alpha}_{i,n}^2} + \hat{\xi}_i \tanh\left(\frac{e_{i,n}}{\gamma_i}\right) + e_{i,n} \\ &+ \text{sign}(e_{i,n})(\bar{\epsilon}_{i,n-1} + \bar{\phi}_{i,n-1} |e_{i,n-1}|) \\ &- \chi_{i,(n-1)2} \end{aligned} \quad (19)$$

where if $j = 2, J_i = A_i$, and if $j = 3, \dots, n - 1, J_i = 1$ and

$$\begin{aligned} M_{i,j}(e_{i,j}) &= \begin{cases} e_{i,j}^{1+\zeta}, & \text{if } e_{i,j} \geq 0 \\ -|e_{i,j}|^{1+\zeta}, & \text{if } e_{i,j} < 0, j = 1, 2, \dots, n \end{cases} \\ N_{i,j}(e_{i,j}) &= \begin{cases} e_{i,j}^{1-\zeta}, & \text{if } e_{i,j} \geq 0 \\ -|e_{i,j}|^{1-\zeta}, & \text{if } e_{i,j} < 0, j = 1, 2, \dots, n \end{cases} \end{aligned} \quad (20)$$

The adaptive laws $\hat{\mu}_i, \hat{\xi}_i$, and $\hat{\lambda}_i$ are constructed as follows

$$\begin{aligned} \dot{\hat{\mu}}_i &= \sum_{j=1}^n \frac{p_i}{2\check{\alpha}_{i,j}^2} e_{i,j}^2 \Phi_{m_{i,j}}^T \Phi_{m_{i,j}} - c_{i,1} \hat{\mu}_i^{1+\zeta} - c_{i,2} \hat{\mu}_i \\ \dot{\hat{\xi}}_i &= \eta_i \left| e_{i,n} \tanh\left(\frac{e_{i,n}}{\gamma_i}\right) \right| - c_{i,1} \hat{\xi}_i^{1+\zeta} - c_{i,2} \hat{\xi}_i \\ \dot{\hat{\lambda}}_i &= \tau_i |e_{i,n} \check{\alpha}_{i,n}| - c_{i,1} \hat{\lambda}_i^{1+2\zeta} - c_{i,2} \hat{\lambda}_i \end{aligned} \quad (21)$$

where $\hat{\mu}_i(0) \geq 0, \hat{\xi}_i(0) \geq 0, \hat{\lambda}_i(0) \geq 0, c_{i,1} = \frac{\pi}{r\zeta T_s}, c_{i,2} = \frac{\pi}{\zeta T_s}, 2T_s$ is the predefined settling time, $r = \min$

$$\left\{ n^{\frac{\zeta}{2}}, \frac{1}{2}^{1+\frac{\zeta}{2}} \frac{1}{p_i} \frac{1}{1+\zeta}, \frac{1}{2}^{1+\frac{\zeta}{2}} \frac{1}{\eta_i} \frac{1}{1+\zeta}, \frac{1}{2}^{1+\frac{\zeta}{2}} \frac{1}{\tau_i} \frac{1}{1+2\zeta} \right\},$$

$\check{\alpha}_{i,j}, p_i, \eta_i, \tau_i, \gamma_i > 0$ and $0 < \zeta < 1$ are designed positive constants, ξ_i and λ_i will be defined later. Moreover, the results obtained from this study are presented as Theorem 1.

Remark 7 By using Lemma 6, since $\hat{\mu}_i(0) \geq 0, \hat{\xi}_i(0) \geq 0, \hat{\lambda}_i(0) \geq 0$, it follows that for $t \geq 0, \hat{\mu}_i(t) \geq 0, \hat{\xi}_i(t) \geq 0, \hat{\lambda}_i(t) \geq 0$. This presents essential conditions for stability analysis in the subsequent sections.

Theorem 1 For NMASs with input quantization and actuator faults satisfying Assumptions 1-5, by utilizing the designed controller (16), virtual controllers (15), and adaptive laws (21), the following conclusions can be drawn

- (1) The tracking errors, denoted as $e_{i,1}$, can converge to a small range within a predefined-time $2T_s$.
- (2) All signals within the closed-loop system remain bounded.

Proof More specifically, this procedure consists of two distinct phases. Initially, the backstepping methodology is employed to formulate the required controller and adaptive laws. Then, leveraging the relevant knowledge presented in Sect. 2, a comprehensive stability analysis of the system is conducted. Next, we present a detailed process for the controller design, which is presented in a recursive fashion. \square

3.1 Control design process

Step 1: A suitable Lyapunov function is chosen as follows

$$V_1 = \sum_{i=1}^N \left(\frac{1}{2} e_{i,1}^2 + \frac{1}{2p_i} \tilde{\mu}_i^2 \right) \tag{22}$$

By considering the system (1) and the coordinate transformation (14), we can calculate the time derivative of the Lyapunov function mentioned above as follows

$$\begin{aligned} \dot{V}_1 = & \sum_{i=1}^N \left[e_{i,1} (A_i (\phi_{i,1} x_{i,2} + d_{i,1}) + F(\mathbf{X}_{i,1})) \right. \\ & \left. - \sum_{k=1}^N a_{i,k} (\phi_{k,1} x_{k,2} + d_{k,1}) - r_i \dot{y}_d \right] - \frac{1}{p_i} \tilde{\mu}_i \dot{\hat{\mu}}_i \end{aligned} \tag{23}$$

where $A_i = \sum_{k=1}^N a_{i,k} + r_i$ and $F(\mathbf{X}_{i,1}) = A_i \sigma_{i,1} - \sum_{k=1}^N a_{i,k} \sigma_{k,1}$ represents an unknown term with $\mathbf{X}_{i,1} = [x_{i,1}, x_{k,1}]^T$. Based on Lemma 4, the unknown term $F(\mathbf{X}_{i,1})$ can be approximated using the MTN as follows

$$F(\mathbf{X}_{i,1}) = \mathbf{H}_{i,1}^T \Phi_{m_{i,1}} + \epsilon_{i,1}, |\epsilon_{i,1}| < \bar{\epsilon}_{i,1} \tag{24}$$

where $\epsilon_{i,1}$ is an approximation error. Naturally, by substituting (24) into (23) and applying the Young's inequality, we obtain

$$\left\{ \begin{aligned} e_{i,1} F(\mathbf{X}_{i,1}) &\leq \frac{\mu_i e_{i,1}^2 \Phi_{m_{i,1}}^T \Phi_{m_{i,1}}}{2\check{a}_{i,1}^2} \\ &\quad + \frac{\check{a}_{i,1}^2 + \bar{\epsilon}_{i,1}^2 + e_{i,1}^2}{2} \\ e_{i,1} A_i d_{i,1} &\leq A_i \left(\frac{1}{2} e_{i,1}^2 + \frac{1}{2} \bar{d}_{i,1}^2 \right) \\ -e_{i,1} \sum_{k=1}^N a_{i,k} d_{k,1} &\leq \sum_{k=1}^N a_{i,k} \left(\frac{1}{2} e_{i,1}^2 + \frac{1}{2} \bar{d}_{k,1}^2 \right) \end{aligned} \right. \tag{25}$$

Next, according to (14) and substitute (25) into (23), yield

$$\begin{aligned} \dot{V}_1 \leq & \sum_{i=1}^N \left[A_i \phi_{i,1} e_{i,1} \alpha_{i,1} + \sum_{k=1}^N a_{i,k} \bar{\phi}_{k,1} |e_{i,1} x_{k,2}| \right. \\ & + \frac{\mu_i e_{i,1}^2 \Phi_{m_{i,1}}^T \Phi_{m_{i,1}}}{2\check{a}_{i,1}^2} + \frac{1 + A_i + \sum_{k=1}^N a_{i,k}}{2} e_{i,1}^2 \\ & + \frac{A_i}{2} \bar{d}_{i,1}^2 + \frac{\sum_{k=1}^N a_{i,k}}{2} \bar{d}_{k,1}^2 + \frac{1}{2} \bar{\epsilon}_{i,1}^2 + \frac{1}{2} \check{a}_{i,1}^2 \\ & \left. - e_{i,1} r_i \dot{y}_d + A_i |\bar{\phi}_{i,1} e_{i,1} e_{i,2}| - \frac{1}{p_i} \tilde{\mu}_i \dot{\hat{\mu}}_i \right] \end{aligned} \tag{26}$$

Subsequently, we substitute the previously designed intermediate virtual controller given by (17) and adaptive laws (21) into (26), the derivative \dot{V}_1 can be reexpressed as follows

$$\begin{aligned} \dot{V}_1 \leq & \sum_{i=1}^N \left[-c_{i,1} \left(\frac{1}{2} e_{i,1}^2 \right)^{1+\frac{\varsigma}{2}} - c_{i,2} \left(\frac{1}{2} e_{i,1}^2 \right)^{1-\frac{\varsigma}{2}} \right. \\ & + \frac{c_{i,1}}{p_i} \tilde{\mu}_i \hat{\mu}_i^{1+\varsigma} + \frac{c_{i,2}}{p_i} \tilde{\mu}_i \hat{\mu}_i + A_i |\bar{\phi}_{i,1} e_{i,1} e_{i,2}| \\ & + \frac{A_i}{2} \bar{d}_{i,1}^2 + \frac{\sum_{k=1}^N a_{i,k}}{2} \bar{d}_{k,1}^2 + \frac{1}{2} \bar{\epsilon}_{i,1}^2 + \frac{1}{2} \check{a}_{i,1}^2 \\ & \left. + A_i \phi_{i,1} e_{i,1} \alpha_{i,1} + e_{i,1} \check{\alpha}_{i,1} \right] \end{aligned} \tag{27}$$

Furthermore, according to the virtual controller (15) and Lemma 7, it can be noted that

$$\begin{aligned} A_i \phi_{i,1} e_{i,1} \alpha_{i,1} &\leq - \frac{e_{i,1}^2 \check{\alpha}_{i,1}^2}{\sqrt{e_{i,1}^2 \check{\alpha}_{i,1}^2 + \varpi_i}} \\ &\leq - |e_{i,1} \check{\alpha}_{i,1}| + \varpi_i \leq \varpi_i - e_{i,1} \check{\alpha}_{i,1} \end{aligned} \tag{28}$$

Then, substituting (28) into (27), one has

$$\begin{aligned} \dot{V}_1 \leq & \sum_{i=1}^N \left[-c_{i,1} \left(\frac{1}{2} e_{i,1}^2 \right)^{1+\frac{\varsigma}{2}} - c_{i,2} \left(\frac{1}{2} e_{i,1}^2 \right)^{1-\frac{\varsigma}{2}} \right. \\ & + \frac{c_{i,1}}{p_i} \tilde{\mu}_i \hat{\mu}_i^{1+\varsigma} + \frac{c_{i,2}}{p_i} \tilde{\mu}_i \hat{\mu}_i \\ & \left. + A_i |\bar{\phi}_{i,1} e_{i,1} e_{i,2}| + \Lambda_{i,1} \right] \end{aligned} \tag{29}$$

where $\Lambda_{i,1} = \frac{A_i}{2} \bar{d}_{i,1}^2 + \frac{\sum_{k=1}^N a_{i,k}}{2} \bar{d}_{k,1}^2 + \frac{1}{2} \bar{\epsilon}_{i,1}^2 + \frac{1}{2} \check{a}_{i,1}^2 + \varpi_i$.

Step j ($2 \leq j \leq n - 1$): In order to estimate the derivative of the virtual controller $\alpha_{i,j-1}$, according to

Lemma 5, we employ the finite time differentiator as follows

$$\begin{cases} \dot{\chi}_{i,(j-1)1} = -\ell_1 \text{sig}(\chi_{i,(j-1)1} - \alpha_{i,j-1}) + \chi_{i,(j-1)2} \\ \dot{\chi}_{i,(j-1)2} = -\ell_2 \text{sign}(\chi_{i,(j-1)2} - \alpha_{i,j-1}) \end{cases} \quad (30)$$

Therefore, $\dot{\alpha}_{i,j-1} = \chi_{i,(j-1)2} + \varepsilon_{i,j-1}$ holds, where $|\varepsilon_{i,j-1}| < \bar{\varepsilon}_{i,j-1}$.

Then, a suitable Lyapunov function is chosen as follows

$$V_j = V_{j-1} + \sum_{i=1}^N \left(\frac{1}{2} e_{i,j}^2 \right) \quad (31)$$

By following the same computational procedure as in step 1 and incorporating the differentiator (30), its derivative with respect to time is given as follows

$$\begin{aligned} \dot{V}_j \leq \dot{V}_{j-1} + \sum_{i=1}^N (e_{i,j} (\phi_{i,j} x_{i,j+1} + d_{i,j} \\ + F(\mathbf{X}_{i,j}) - \chi_{i,(j-1)2} + \bar{\varepsilon}_{i,j-1})) \end{aligned} \quad (32)$$

where $F(\mathbf{X}_{i,j}) = \sigma_{i,j}$ represents an unknown term with $\mathbf{X}_{i,j} = [x_{i,1}, x_{i,2}, \dots, x_{i,j}]^T$. Similarity to step 1, the unknown term $F(\mathbf{X}_{i,j})$ can be approximated using the MTN as follows

$$F(\mathbf{X}_{i,j}) = \mathbf{H}_{i,j}^T \Phi_{m_{i,j}} + \epsilon_{i,j}, |\epsilon_{i,j}| < \bar{\epsilon}_{i,j} \quad (33)$$

where $\epsilon_{i,j}$ is an approximation error. Naturally, by substituting (33) into (32) and applying the Young's inequality, we obtain

$$\begin{cases} e_{i,j} F(\mathbf{X}_{i,j}) \leq \frac{\mu_i e_{i,j}^2 \Phi_{m_{i,j}}^T \Phi_{m_{i,j}}}{2\check{a}_{i,j}^2} \\ \quad + \frac{1}{2} \check{a}_{i,j}^2 + \frac{1}{2} \bar{\epsilon}_{i,j}^2 + \frac{1}{2} e_{i,j}^2 \\ e_{i,j} d_{i,j} \leq \frac{1}{2} e_{i,j}^2 + \frac{1}{2} \bar{d}_{i,j}^2 \end{cases} \quad (34)$$

Next, according to (14) and substitute (34) into (32), yield

$$\begin{aligned} \dot{V}_j \leq \dot{V}_{j-1} + \sum_{i=1}^N e_{i,j} \phi_{i,j} \alpha_{i,j} + \sum_{i=1}^N [|\bar{\phi}_{i,j} e_{i,j} e_{i,j+1}| \\ + e_{i,j}^2 + \frac{\mu_i e_{i,j}^2 \Phi_{m_{i,j}}^T \Phi_{m_{i,j}}}{2\check{a}_{i,j}^2} + |e_{i,j}| \bar{\varepsilon}_{i,j-1} \\ - e_{i,j} \chi_{i,(j-1)2} + \frac{1}{2} \check{a}_{i,j}^2 + \frac{1}{2} \bar{\epsilon}_{i,j}^2 + \frac{1}{2} \bar{d}_{i,j}^2] \end{aligned} \quad (35)$$

Subsequently, similar to step 1, we substitute the previously designed virtual controllers given by (15), (18) and adaptive laws (21) into (35), the derivative \dot{V}_j can be reexpressed as follows

$$\begin{aligned} \dot{V}_j \leq \sum_{i=1}^N \left[-c_{i,1} \sum_{\lambda=1}^j \left(\frac{1}{2} e_{i,\lambda}^2 \right)^{1+\frac{\xi}{2}} - c_{i,2} \sum_{\lambda=1}^j \left(\frac{1}{2} e_{i,\lambda}^2 \right)^{1-\frac{\xi}{2}} \right. \\ \left. + \frac{c_{i,1}}{p_i} \tilde{\mu}_i \hat{\mu}_i^{1+\varsigma} + \frac{c_{i,2}}{p_i} \tilde{\mu}_i \hat{\mu}_i \right. \\ \left. + |\bar{\phi}_{i,j} e_{i,j} e_{i,j+1}| + \Lambda_{i,j} \right] \end{aligned} \quad (36)$$

where $\Lambda_{i,j} = \Lambda_{i,j-1} + \frac{1}{2} \check{a}_{i,j}^2 + \frac{1}{2} \bar{\epsilon}_{i,j}^2 + \frac{1}{2} \bar{d}_{i,j}^2 + \varpi_i$.

Step n : Similar to step j , we employ the finite-time differentiator to estimate the derivative of the virtual controller $\alpha_{i,n-1}$, where $\dot{\alpha}_{i,n-1} = \chi_{i,(n-1)2} + \varepsilon_{i,n-1}$ with $|\varepsilon_{i,n-1}| < \bar{\varepsilon}_{i,n-1}$. From Assumptions 3-5, we can obtain

$$\sum_{l=1}^{m_i} |\phi_{i,nl}| \varrho_{i,lh} \geq \min \left\{ |\phi_{i,n1}| \varrho_{i,1h}, \dots, |\phi_{i,nm_i}| \varrho_{i,m_ih} \right\} > 0.$$

So, it is easy for us to obtain $\inf_{t \geq 0} \sum_{l=1}^{m_i} |\phi_{i,nl}| \varrho_{i,lh} \geq \min \left\{ |\phi_{i,n1}| \varrho_{i,1h}, \dots, |\phi_{i,nm_i}| \varrho_{i,m_ih} \right\} > 0$. To compensate for the effects of input quantization and actuator faults, according to faults model (3) and Lemma 3, we define

$$\check{h}_i = \inf_{t \geq 0} \sum_{l=1}^{m_i} |\phi_{i,nl}| \varrho_{i,lh}, \quad \lambda_i = \frac{1}{\check{h}_i} \quad (37)$$

$$\xi_i = \sup_{t \geq 0} \sum_{l=1}^{m_i} \phi_{i,nl} (\varrho_{i,lh} R_{i,l} + \bar{u}_{i,lh})$$

Then, a suitable Lyapunov function is chosen as follows

$$V_n = V_{n-1} + \sum_{i=1}^N \left(\frac{1}{2} e_{i,n}^2 + \frac{\check{h}_i}{2\tau_i} \tilde{\lambda}_i^2 + \frac{1}{2\eta_i} \tilde{\xi}_i^2 \right) \quad (38)$$

Building upon the previous steps and incorporating Lemma 3, its derivative with respect to time is given as follows

$$\begin{aligned} \dot{V}_n \leq \dot{V}_{n-1} + \sum_{i=1}^N \left[e_{i,n} \sum_{l=1}^{m_i} \phi_{i,nl} (\varrho_{i,lh} P(u_{i,l}) u_{i,l} \right. \\ \left. + \varrho_{i,lh} R_{i,l} + \bar{u}_{i,lh}) + e_{i,n} F(\mathbf{X}_{i,n}) + e_{i,n} d_{i,n} \right. \\ \left. - e_{i,n} \chi_{i,(n-1)2} + |e_{i,n}| \bar{\varepsilon}_{i,n-1} - \frac{\check{h}_i}{\tau_i} \tilde{\lambda}_i \dot{\lambda}_i - \frac{1}{\eta_i} \tilde{\xi}_i \dot{\xi}_i \right] \end{aligned} \quad (39)$$

Similar to the step j , $F(\mathbf{X}_{i,n}) = \sigma_{i,n}$ represents an unknown term with $\mathbf{X}_{i,n} = [x_{i,1}, x_{i,2}, \dots, x_{i,n}]^T$, the

unknown term $F(X_{i,n})$ can be approximated using the MTN as follows

$$F(X_{i,n}) = H_{i,n}^T \Phi_{m_{i,n}} + \epsilon_{i,n}, \quad |\epsilon_{i,n}| < \bar{\epsilon}_{i,n} \tag{40}$$

where $\epsilon_{i,n}$ is an approximation error. Naturally, by substituting (40) into (39) and applying the Young's inequality, we obtain

$$\left\{ \begin{aligned} e_{i,n} F(X_{i,n}) &\leq \frac{\mu_i e_{i,n}^2 \Phi_{m_{i,n}}^T \Phi_{m_{i,n}}}{2\bar{a}_{i,n}^2} \\ &\quad + \frac{1}{2}\bar{a}_{i,n}^2 + \frac{1}{2}\bar{\epsilon}_{i,n}^2 + \frac{1}{2}e_{i,n}^2 \\ e_{i,n} d_{i,n} &\leq \frac{1}{2}e_{i,n}^2 + \frac{1}{2}\bar{d}_{i,n}^2 \end{aligned} \right. \tag{41}$$

Next, by substituting (41) into (39) and according to (37), yielding

$$\begin{aligned} \dot{V}_n &\leq \dot{V}_{n-1} + \sum_{i=1}^N \left[e_{i,n} \sum_{l=1}^{m_i} \phi_{i,nl} \varrho_{i,ln} P(u_{i,l}) u_{i,l} + |e_{i,n}| \xi_i \right. \\ &\quad + \frac{\mu_i e_{i,n}^2 \Phi_{m_{i,n}}^T \Phi_{m_{i,n}}}{2\bar{a}_{i,n}^2} + \frac{1}{2}\bar{a}_{i,n}^2 + \frac{1}{2}\bar{\epsilon}_{i,n}^2 - e_{i,n} \chi_{i,(n-1)2} \\ &\quad \left. + e_{i,n}^2 + \frac{1}{2}\bar{d}_{i,n}^2 + |e_{i,n}| \bar{\epsilon}_{i,n-1} - \frac{\hbar_i}{\tau_i} \tilde{\lambda}_i \hat{\lambda}_i - \frac{1}{\eta_i} \tilde{\xi}_i \hat{\xi}_i \right] \end{aligned} \tag{42}$$

Subsequently, we substitute the previously designed auxiliary virtual signal given by (19) and adaptive laws (21) into (42), the derivative \dot{V}_n can be reexpressed as follows

$$\begin{aligned} \dot{V}_n &\leq \sum_{i=1}^N \left[-c_{i,1} \sum_{\tilde{\lambda}=1}^n \left(\frac{1}{2} e_{i,\tilde{\lambda}}^2 \right)^{1+\frac{\xi}{2}} - c_{i,2} \sum_{\tilde{\lambda}=1}^n \left(\frac{1}{2} e_{i,\tilde{\lambda}}^2 \right)^{1-\frac{\xi}{2}} \right. \\ &\quad + \frac{c_{i,1}}{p_i} \tilde{\mu}_i \hat{\mu}_i^{1+\varsigma} + \frac{c_{i,2}}{p_i} \tilde{\mu}_i \hat{\mu}_i + \frac{c_{i,1}}{\eta_i} \tilde{\xi}_i \hat{\xi}_i^{1+\varsigma} + \frac{c_{i,2}}{\eta_i} \tilde{\xi}_i \hat{\xi}_i \\ &\quad + \frac{c_{i,1} \hbar_i}{\tau_i} \tilde{\lambda}_i \hat{\lambda}_i^{1+2\varsigma} + \frac{c_{i,2} \hbar_i}{\tau_i} \tilde{\lambda}_i \hat{\lambda}_i + \frac{1}{2} \bar{d}_{i,n}^2 + \frac{1}{2} \bar{a}_{i,n}^2 + \frac{1}{2} \bar{\epsilon}_{i,n}^2 \\ &\quad + \xi_i \left(|e_{i,n}| - e_{i,n} \tanh \left(\frac{e_{i,n}}{\gamma_i} \right) \right) - |e_{i,n} \check{\alpha}_{i,n}| \hbar_i \tilde{\lambda}_i \\ &\quad \left. + e_{i,n} \sum_{l=1}^{m_i} \phi_{i,nl} \varrho_{i,ln} P(u_{i,l}) u_{i,l} + e_{i,n} \check{\alpha}_{i,n} \right] \end{aligned} \tag{43}$$

Furthermore, according to Lemma 7 and in conjunction with (16) and (37), it can be observed that

$$\begin{aligned} e_{i,n} \sum_{l=1}^{m_i} \phi_{i,nl} \varrho_{i,ln} P(u_{i,l}) u_{i,l} &\leq - \sum_{l=1}^{m_i} |\phi_{i,nl}| \varrho_{i,ln} \frac{e_{i,n}^2 \hat{\lambda}_i^2 \check{\alpha}_{i,n}^2}{\sqrt{e_{i,n}^2 \hat{\lambda}_i^2 \check{\alpha}_{i,n}^2 + \varpi_i^2}} \\ &\leq - \frac{\hbar_i e_{i,n}^2 \hat{\lambda}_i^2 \check{\alpha}_{i,n}^2}{\sqrt{e_{i,n}^2 \hat{\lambda}_i^2 \check{\alpha}_{i,n}^2 + \varpi_i^2}} \leq \hbar_i \varpi_i - |e_{i,n} \check{\alpha}_{i,n}| \hbar_i \hat{\lambda}_i \end{aligned} \tag{44}$$

Then, by substituting (44) into (43) and utilizing the inequality $\xi_i \left(|e_{i,n}| - e_{i,n} \tanh \left(\frac{e_{i,n}}{\gamma_i} \right) \right) \leq 0.2785 \xi_i \gamma_i$, we obtain

$$\begin{aligned} \dot{V}_n &\leq \sum_{i=1}^N \left[-c_{i,1} \sum_{\tilde{\lambda}=1}^n \left(\frac{1}{2} e_{i,\tilde{\lambda}}^2 \right)^{1+\frac{\xi}{2}} - c_{i,2} \sum_{\tilde{\lambda}=1}^n \left(\frac{1}{2} e_{i,\tilde{\lambda}}^2 \right)^{1-\frac{\xi}{2}} \right. \\ &\quad + \frac{c_{i,1}}{p_i} \tilde{\mu}_i \hat{\mu}_i^{1+\varsigma} + \frac{c_{i,2}}{p_i} \tilde{\mu}_i \hat{\mu}_i + \frac{c_{i,1}}{\eta_i} \tilde{\xi}_i \hat{\xi}_i^{1+\varsigma} \\ &\quad \left. + \frac{c_{i,2}}{\eta_i} \tilde{\xi}_i \hat{\xi}_i + \frac{c_{i,1} \hbar_i}{\tau_i} \tilde{\lambda}_i \hat{\lambda}_i^{1+2\varsigma} + \frac{c_{i,2} \hbar_i}{\tau_i} \tilde{\lambda}_i \hat{\lambda}_i + \Lambda_{i,n} \right] \end{aligned} \tag{45}$$

where $\Lambda_{i,n} = \Lambda_{i,n-1} + \frac{1}{2} \bar{a}_{i,n}^2 + \frac{1}{2} \bar{\epsilon}_{i,n}^2 + \frac{1}{2} \bar{d}_{i,n}^2 + \hbar_i \varpi_i + 0.2785 \xi_i \gamma_i$.

Remark 8 Although the literatures [48,49] addresses actuator failures, the discussed fault models are limited to cases where the number of occurrences per actuator failure is finite. While [50] also deals with actuator failures occurring an infinite number of times, the modular approach it employs typically necessitates prior knowledge of the uncertainty bounds caused by faults and system parameters. In contrast, this paper adopts a boundary estimation method to estimate the boundaries of unknown terms induced by actuator failures. Unlike modular approaches, this method does not require any prior knowledge of uncertainty constraints.

3.2 Stability analysis

Next, we proceed with the stability analysis of the system. According to Lemma 10, one has

$$-c_{i,1} \sum_{j=1}^n \left(\frac{1}{2} e_{i,j}^2 \right)^{1+\frac{\xi}{2}} \leq -\frac{c_{i,1}}{n^{\frac{\xi}{2}}} \left(\sum_{j=1}^n \frac{1}{2} e_{i,j}^2 \right)^{1+\frac{\xi}{2}} \tag{46}$$

$$-c_{i,2} \sum_{j=1}^n \left(\frac{1}{2} e_{i,j}^2\right)^{1-\frac{\xi}{2}} \leq -c_{i,2} \left(\sum_{j=1}^n \frac{1}{2} e_{i,j}^2\right)^{1-\frac{\xi}{2}} \quad (47)$$

In dealing with $\tilde{\mu}_i \hat{\mu}_i$, we first apply the Young’s inequality, one has

$$\frac{c_{i,2}}{p_i} \tilde{\mu}_i \hat{\mu}_i \leq -\frac{c_{i,2}}{2p_i} \tilde{\mu}_i^2 + \frac{c_{i,2}}{2p_i} \mu_i^2 \quad (48)$$

Then, using Lemma 8 and defining $x = 1, y = \frac{\tilde{\mu}_i^2}{2p_i}$, $a_f = \frac{\xi}{2}, b_f = 1 - \frac{\xi}{2}$ and $\delta_f = \exp\left(\left(\frac{2-\xi}{\xi}\right)\ln\left(\frac{2-\xi}{2}\right)\right)$, we have

$$c_{i,2} \left(\frac{1}{2p_i} \tilde{\mu}_i^2\right)^{1-\frac{\xi}{2}} \leq \frac{c_{i,2}}{2p_i} \tilde{\mu}_i^2 + c_{i,2} \frac{\xi}{2} \left(\frac{2-\xi}{2}\right)^{\frac{2-\xi}{\xi}} \quad (49)$$

Next, substituting (49) into (48), we have

$$\begin{aligned} \frac{c_{i,2}}{p_i} \tilde{\mu}_i \hat{\mu}_i &\leq -c_{i,2} \left(\frac{1}{2p_i} \tilde{\mu}_i^2\right)^{1-\frac{\xi}{2}} \\ &\quad + \frac{c_{i,2}}{2p_i} \mu_i^2 + c_{i,2} \frac{\xi}{2} \left(\frac{2-\xi}{2}\right)^{\frac{2-\xi}{\xi}} \end{aligned} \quad (50)$$

Regarding the term $\tilde{\mu}_i \hat{\mu}_i^{1+\xi}$, according to Lemma 9, we have

$$\begin{aligned} \frac{c_{i,1}}{p_i} \tilde{\mu}_i \hat{\mu}_i^{1+\xi} &\leq \frac{c_{i,1}}{p_i} \tilde{\mu}_i (\mu_i - \tilde{\mu}_i)^{1+\xi} \\ &\leq \frac{c_{i,1}}{p_i} \frac{1+\xi}{2+\xi} (\mu_i^{2+\xi} - \tilde{\mu}_i^{2+\xi}) \\ &\leq -c_{i,1} \left(2^{1+\frac{\xi}{2}} p_i^{\frac{\xi}{2}}\right) \frac{1+\xi}{2+\xi} \left(\frac{1}{2p_i} \tilde{\mu}_i^2\right)^{1+\frac{\xi}{2}} \\ &\quad + \frac{c_{i,1}}{p_i} \frac{1+\xi}{2+\xi} \mu_i^{2+\xi} \end{aligned} \quad (51)$$

Naturally, by employing the same scaling method as above, we can obtain

$$\begin{aligned} \frac{c_{i,2}}{\eta_i} \tilde{\xi}_i \hat{\xi}_i &\leq -c_{i,2} \left(\frac{1}{2\eta_i} \tilde{\xi}_i^2\right)^{1-\frac{\xi}{2}} \\ &\quad + \frac{c_{i,2}}{2\eta_i} \tilde{\xi}_i^2 + c_{i,2} \frac{\xi}{2} \left(\frac{2-\xi}{2}\right)^{\frac{2-\xi}{\xi}} \end{aligned} \quad (52)$$

$$\begin{aligned} \frac{c_{i,2} \hat{h}_i}{\tau_i} \tilde{\lambda}_i \hat{\lambda}_i &\leq -c_{i,2} \left(\frac{\hat{h}_i}{2\tau_i} \tilde{\lambda}_i^2\right)^{1-\frac{\xi}{2}} \\ &\quad + \frac{c_{i,2} \hat{h}_i}{\tau_i} \tilde{\lambda}_i^2 + c_{i,2} \frac{\xi}{2} \left(\frac{2-\xi}{2}\right)^{\frac{2-\xi}{\xi}} \end{aligned} \quad (53)$$

$$\begin{aligned} \frac{c_{i,1}}{\eta_i} \tilde{\xi}_i \hat{\xi}_i^{1+\xi} &\leq -c_{i,1} \left(2^{1+\frac{\xi}{2}} \eta_i^{\frac{\xi}{2}}\right) \frac{1+\xi}{2+\xi} \left(\frac{1}{2\eta_i} \tilde{\xi}_i^2\right)^{1+\frac{\xi}{2}} \\ &\quad + \frac{c_{i,1}}{\eta_i} \frac{1+\xi}{2+\xi} \xi_i^{2+\xi} \end{aligned} \quad (54)$$

$$\begin{aligned} \frac{c_{i,1} \hat{h}_i}{\tau_i} \tilde{\lambda}_i \hat{\lambda}_i^{1+2\xi} &\leq -c_{i,1} 2^{1+\frac{\xi}{2}} \tau_i^{\frac{\xi}{2}} \frac{1+2\xi}{2+2\xi} \left(\frac{\hat{h}_i}{2\tau_i} \tilde{\lambda}_i^2\right)^{1+\frac{\xi}{2}} \\ &\quad + \frac{c_{i,1} \hat{h}_i}{\tau_i} \frac{1+2\xi}{2+2\xi} \lambda_i^{2+2\xi} \\ &\quad + c_{i,1} \frac{1+2\xi}{2+2\xi} \frac{\xi}{2(1+\xi)} \left(\frac{2(1+\xi)}{2+\xi}\right)^{-\frac{2+\xi}{\xi}} \left(\frac{\hat{h}_i}{\tau_i}\right)^{2+\xi} \end{aligned} \quad (55)$$

Then, substituting (46), (47), (50), (51), (52), (53), (54) and (55) into (45) and based on the previous definitions of r , we obtain

$$\dot{V}_n \leq -rc_{i,1} V_n^{1+\frac{\xi}{2}} - c_{i,2} V_n^{1-\frac{\xi}{2}} + \Gamma \quad (56)$$

where $\Gamma = 3c_{i,2} \frac{\xi}{2} \left(\frac{2-\xi}{2}\right)^{\frac{2-\xi}{\xi}}$

$$\begin{aligned} &+ c_{i,1} \frac{1+2\xi}{2+2\xi} \frac{\xi}{2(1+\xi)} \left(\frac{2(1+\xi)}{2+\xi}\right)^{-\frac{2+\xi}{\xi}} \left(\frac{\hat{h}_i}{\tau_i}\right)^{2+\xi} + \frac{c_{i,2}}{2p_i} \mu_i^2 + \\ &+ \frac{c_{i,1}}{p_i} \frac{1+\xi}{2+\xi} \mu_i^{2+\xi} + \frac{c_{i,2}}{2\eta_i} \xi_i^2 + \frac{c_{i,2} \hat{h}_i}{2\tau_i} \lambda_i^2 + \frac{c_{i,1}}{\eta_i} \frac{1+\xi}{2+\xi} \xi_i^{2+\xi} + \\ &+ \frac{c_{i,1}}{\tau_i} \frac{1+2\xi}{2+2\xi} \lambda_i^{2+2\xi} + \Lambda_{i,n}. \end{aligned}$$

Subsequently, based on the previous definitions of $c_{i,1}$ and $c_{i,2}$, we have

$$\dot{V}_n \leq -\frac{\pi}{\xi T_s} \left(V_n^{1+\frac{\xi}{2}} + V_n^{1-\frac{\xi}{2}}\right) + \Gamma \quad (57)$$

Based on Lemma 2, it can be concluded that with the implementation of the control law (16) and the parameter adaptive laws (21), the tracking errors of system (1) converge to a small neighborhood within a predefined time interval of $2T_s$, and V_n can remain within the range $\frac{\xi \Gamma T_s}{\pi}$. Subsequently, based on the boundedness of V_n , it can be concluded that $e_{i,j}, \mu_i, \lambda_i$, and ξ_i are bounded. Moreover, as a result, $u_{i,l}, \check{\alpha}_{i,j}$, and $\alpha_{i,j}$ are also bounded. By applying the aforementioned analysis, it can be concluded that all signals are bounded. Thus, the proof is completed.

Remark 9 The parameter selection and system’s initial condition guide of the controllers is as follows: (1) In theory, to improve convergence accuracy, ϖ_i should be minimized. However, excessively small values of ϖ_i can cause $\frac{x^2}{\sqrt{x^2 + \varpi^2}}$ to behave like a sign function, leading to pronounced oscillations in control inputs. (2) To boost parameter update rate, p_i, η_i , and τ_i should be increased, while $\check{a}_{i,j}$ should be decreased. Nevertheless, overly large values of $\frac{p_i}{2\check{a}_{i,j}}, \eta_i$, or τ_i may lead to parameter drift issues. (3) In practical applications, it’s necessary to design a relatively small T_s based on actual requirements to achieve rapid system stabilization. The smaller the T_s , the faster the convergence speed, but this entails significant input consumption,

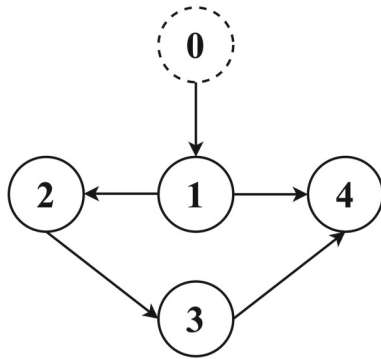


Fig. 1 Communication graph

especially in the initial stages. (4) For $c_{i,1} = \frac{\pi}{r\zeta T_s}$ and $c_{i,2} = \frac{\pi}{\zeta T_s}$, selecting a smaller ζ amplifies $c_{i,1}$ and $c_{i,2}$, thereby accelerating convergence. However, excessively large values of $c_{i,1}$ and $c_{i,2}$ expedite the convergence of parameters $\hat{\mu}$, $\hat{\xi}$, and $\hat{\lambda}$ towards zero. (5) The predefined-time consensus scheme studied in this paper does not rely on initial conditions, thus allowing users to freely select them. However, excessively large initial conditions of the system state can lead to high inputs. Overall, in practical applications, system performance can be improved by selecting appropriate parameters. It should be noted that it may require multiple attempts to achieve the optimal control effect.

4 Simulation results

To provide a more visual demonstration of the theoretical results mentioned above, this section presents two simulation examples.

Example 1 Consider input-quantized NMASs with actuator faults. The communication topology adheres to Assumption 2, as shown in Fig. 1. From the figure, we

can define that $\mathcal{L} = \begin{bmatrix} 0 & 0 & 0 & 0 \\ -1 & 1 & 0 & 0 \\ -1 & 0 & 1 & 0 \\ -1 & 0 & -1 & 2 \end{bmatrix}$, and the dynamic

model of the follower agents i is described as follows

$$\begin{cases} \dot{x}_{i,1} = x_{i,2} + 0.8x_{i,1}^3 \\ \dot{x}_{i,2} = q^f(u_{i,1}) + q^f(u_{i,2}) - 2x_{i,1}^2 + x_{i,2}^3 + \cos(t) \end{cases} \quad (58)$$

The faults model are as follows

$$q_{i,1}^f = \begin{cases} 0.5q(u_{i,1}), & \text{if } t \in [jT^*, (j+1)T^*) \\ q(u_{i,1}), & \text{otherwise} \end{cases} \quad (59)$$

$$q_{i,2}^f = \begin{cases} \sin(t), & \text{if } t \in [jT^*, (j+1)T^*) \\ q(u_{i,2}), & \text{otherwise} \end{cases} \quad (60)$$

where $j = 1, 2, \dots, T^* = 2$. The output reference for the leader is given as $y_d = 0.6 \sin(2t)$. The initial values of all agent systems are set to $\bar{x}_{12}(0) = [0.02, 0.8]^T$, $\bar{x}_{22}(0) = [0.01, 1]^T$, $\bar{x}_{32}(0) = [0.01, 0.09]^T$, $\bar{x}_{42}(0) = [0, 0.7]^T$. Our control objective is to utilize the proposed controller (16), the virtual controller (15), and the adaptive laws (21) to enable the follower agents to track the leader's reference y_d within a predefined-time. Additionally, it is ensured that all signals within the closed-loop system are bounded. To achieve this objective, we choose the following parameters: $T_s = 2$, $\check{a}_{i,1} = 90$, $\check{a}_{i,2} = 90$, $\zeta = 0.1$, $p_i = 80$, $\tau_i = 50$, $\eta_i = 50$, $\ell_1 = 1$, $\ell_2 = 1$, $\rho_{i,l} = 0.9$, $u_{i,l \min} = 0.01$, $\varpi_i = 0.1e^{-0.7t}$, $i = 1, 2, 3, 4$, $l = 1, 2$. To underscore the flexibility of the proposed control scheme, we have adjusted the simulation convergence time T_s to 1, while keeping the integrity of other control parameters and fault models unchanged.

The simulation results are shown in Figs. 2, 3, 4, 5, 6, 7. From Fig. 2, it is evident that the agents output y_i can track the leader signal y_d within the predefined-time 4s. In Fig. 7, with no changes to any parameters or scenarios but only an adjustment of the settling time T_s to 1, there is a notable improvement in tracking performance compared to Fig. 2. Moreover, it achieves a steady state within 2s. Figures 3, 4, 5 illustrate the trajectory of system inputs and inputs quantization. The results indicate that despite intermittent faults, the system can still achieve the desired performance.

Example 2 To illustrate the practical application of our control scheme, we present a model of four single-link manipulators [37] as

$$\begin{cases} \dot{v}_i = q_i \\ M_i \ddot{q}_i + 0.5m_i g l_i \sin q_i = q^f(u_{i,1}) + q^f(u_{i,2}) \end{cases} \quad (61)$$

where $i = 1, 2, 3, 4$, $M_i = 1 \text{ kg} \cdot \text{m}^2$ and $m_i = 1 \text{ kg}$ represent the inertia and mass of the link, respectively.

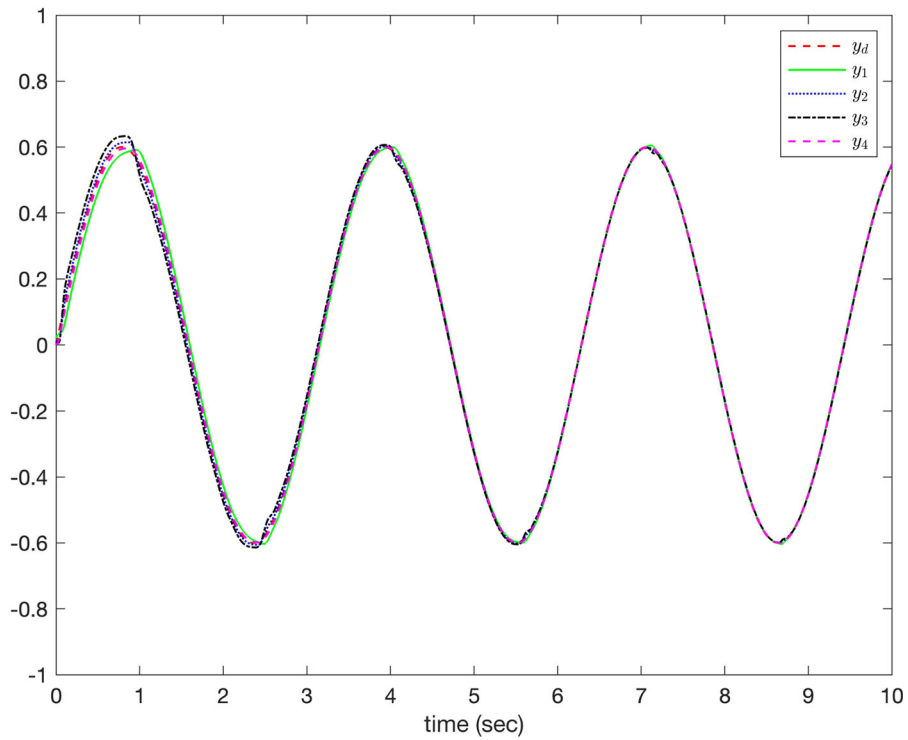


Fig. 2 The trajectories of y_1, y_2, y_3, y_4 and y_d with $T_s = 2$

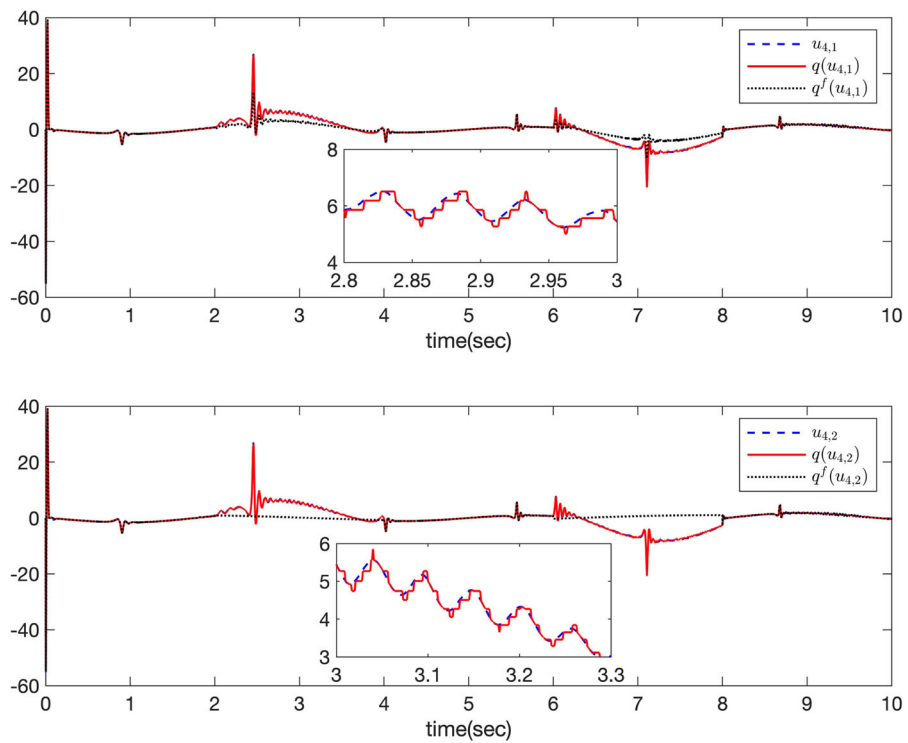


Fig. 3 The trajectories of $u_{1,1}, u_{1,2}, q_{1,1}, q_{1,2}, q^f(u_{1,1}), q^f(u_{1,2})$ with $T_s = 2$

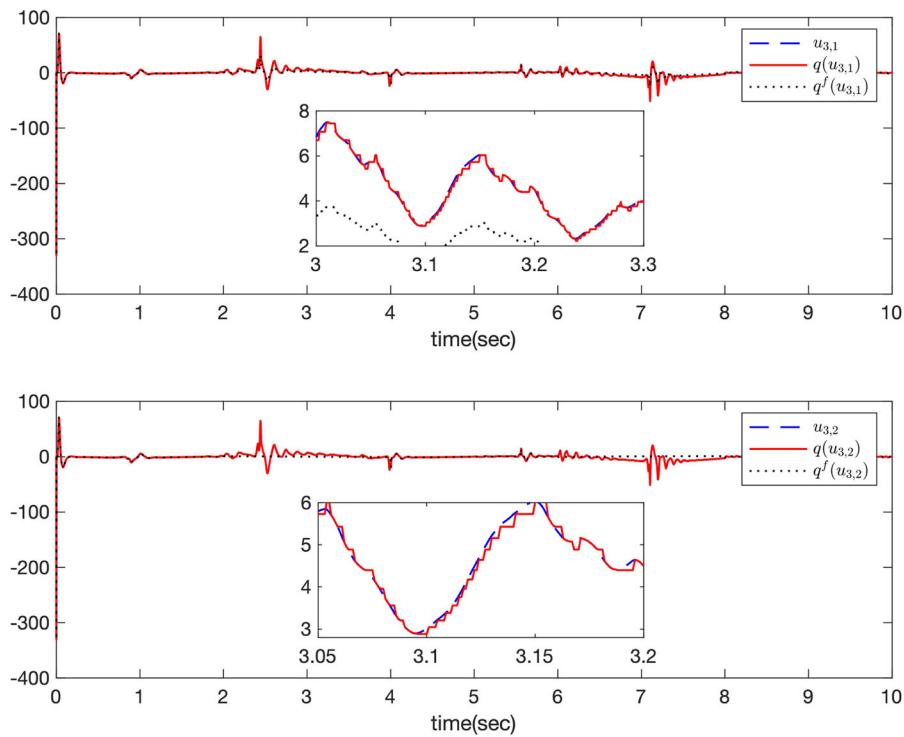


Fig. 4 The trajectories of $u_{2,1}$, $u_{2,2}$, $q_{2,1}$, $q_{2,2}$, $q^f(u_{2,1})$, $q^f(u_{2,2})$ with $T_s = 2$

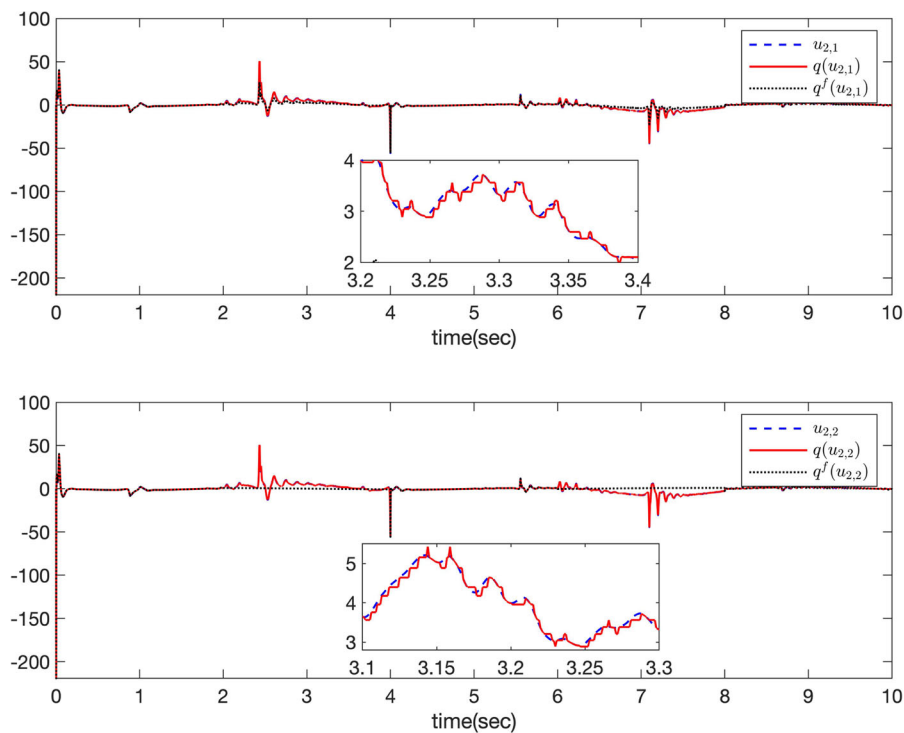


Fig. 5 The trajectories of $u_{3,1}$, $u_{3,2}$, $q_{3,1}$, $q_{3,2}$, $q^f(u_{3,1})$, $q^f(u_{3,2})$ with $T_s = 2$

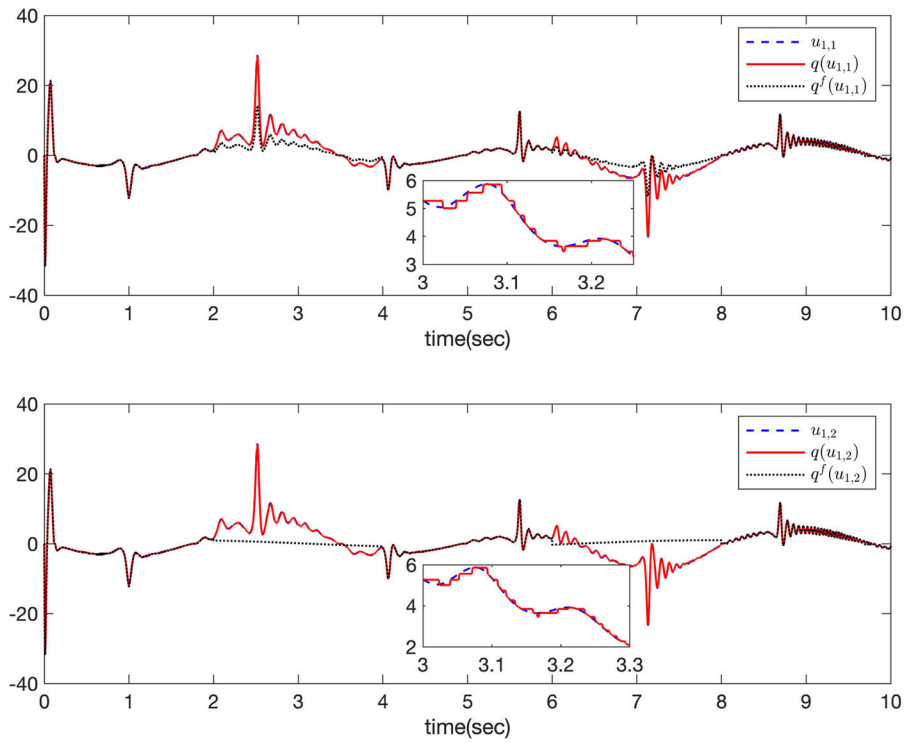


Fig. 6 The trajectories of $u_{4,1}, u_{4,2}, q_{4,1}, q_{4,2}, q^f(u_{4,1}), q^f(u_{4,2})$ with $T_s = 2$

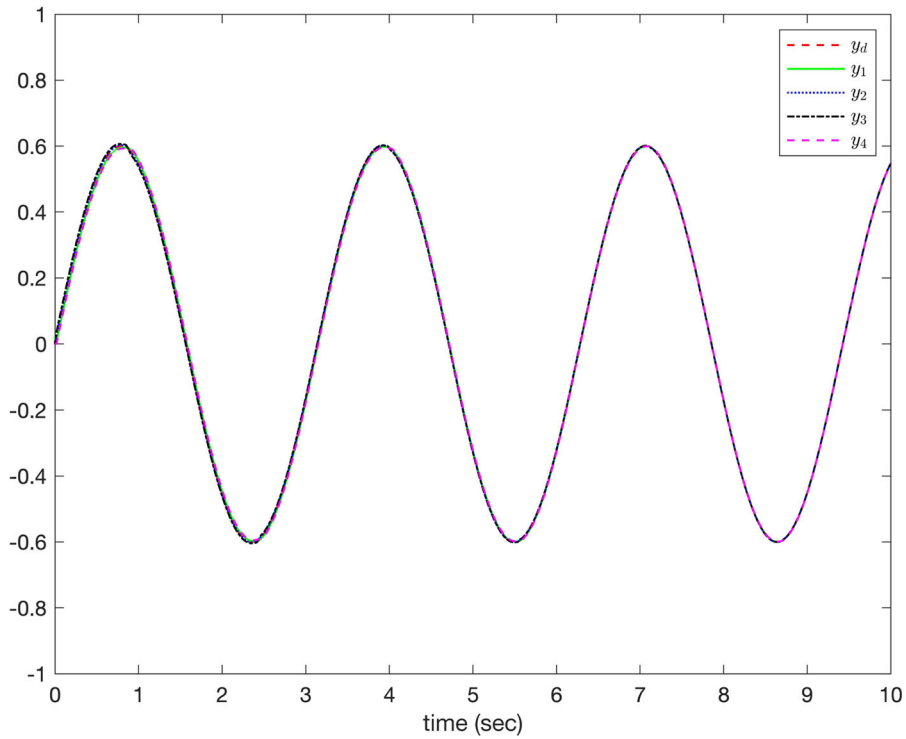


Fig. 7 The trajectories of y_1, y_2, y_3, y_4 and y_d with $T_s = 1$

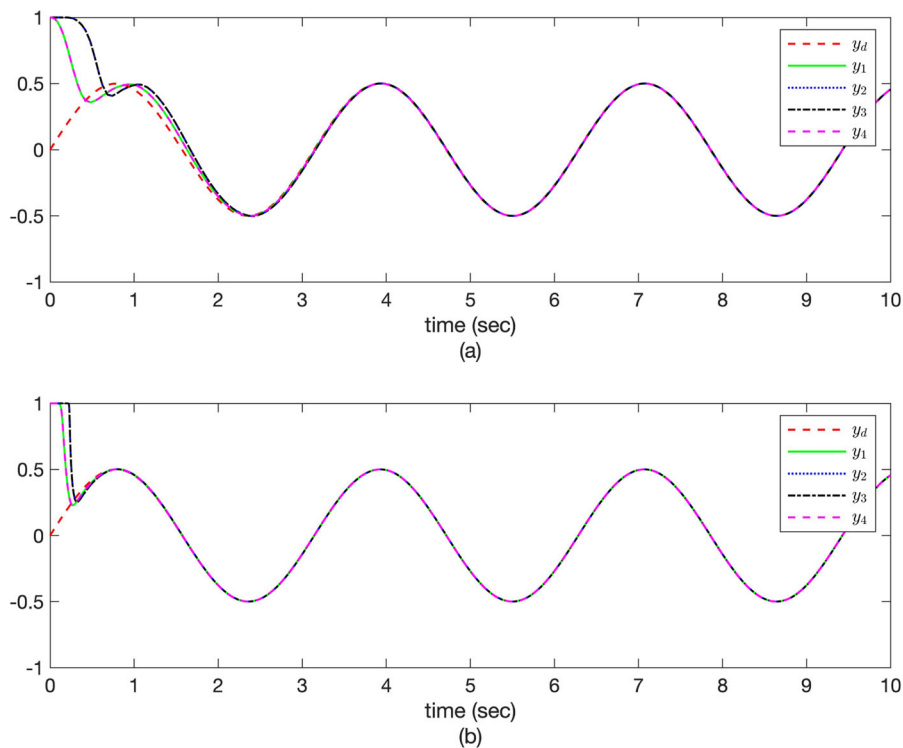


Fig. 8 The trajectories of y_1, y_2, y_3, y_4 and y_d . **a** The prescribed-time consensus scheme in [39]. **b** The predefined-time consensus scheme in this paper

$g = 10\text{m/s}^2, l_i = 1\text{m}, q_m, \dot{q}_m,$ and \ddot{q}_m denote the angular position, angular velocity, and angular acceleration of the link, respectively. $q^f(u_{i,1})$ and $q^f(u_{i,2})$ represent the control forces applied to the link. Additionally, the communication topology, chosen fault parameters are the same as in Example 1. The leader's reference signal is chosen as $y_d = 0.5 \sin(2t)$, the initial values of the system are set as $x_{i,1}(0) = 1$ and $x_{i,2}(0) = 2$, and the system parameters are selected as $T_s = 0.5$, $\check{a}_{i,1} = 100$, $\check{a}_{i,2} = 120$, $\zeta = 0.6$, $p_i = 30$, $\tau_i = 30$, $\eta_i = 30$, $\ell_1 = 1$, $\ell_2 = 1$, $\rho_{i,l} = 0.9$, $u_{i,l \min} = 0.01$, $\varpi_i = 0.1e^{-0.7t}$, $i = 1, 2, 3, 4, l = 1, 2$.

In order to emphasize the superiority of the proposed control protocol, in this instance, we deviate from adjusting the parameters T_s of the control scheme itself, unlike the numerical examples. Instead, we draw from the prescribed-time control scheme in [39], selecting the following parameters as $T_s = 1$, $c_{i,1} = 10$, $c_{i,2} = 9$, $\ell_1 = 1$, $\ell_2 = 1$, $\rho_{i,l} = 0.9$, $u_{i,l \min} = 0.01$, $\varpi_i = 0.1e^{-0.7t}$, $i = 1, 2, 3, 4, l = 1, 2$. Under the condition of adjusting the settling time to be the same, it compares the control performance of the two methods.

The simulation results are shown in Figs. 8, 9, 10, 11, 12. The first graph in Fig. 8 represents the prescribed-time control scheme, while the second graph depicts the predefined-time control scheme. It is evident from both graphs that the response speed of the prescribed-time control scheme is slower compared to the proposed scheme in this paper. The control effect of the proposed control scheme presented in this paper demonstrates a clear advantage. Figures 9, 10, 11, 12 depict the trajectories of system inputs and inputs quantization. Despite the presence of actuator faults, the system is still able to achieve commendable tracking performance.

5 Conclusion

This paper primarily investigates the problem of predefined-time consensus control for NMASSs with actuator faults and input quantization. Firstly, the MTN is employed to approximate the unknown nonlinear functions in NMASSs. Then, to effectively tackle the challenges posed by input quantization and actuator faults, adaptive laws are devised to estimate the

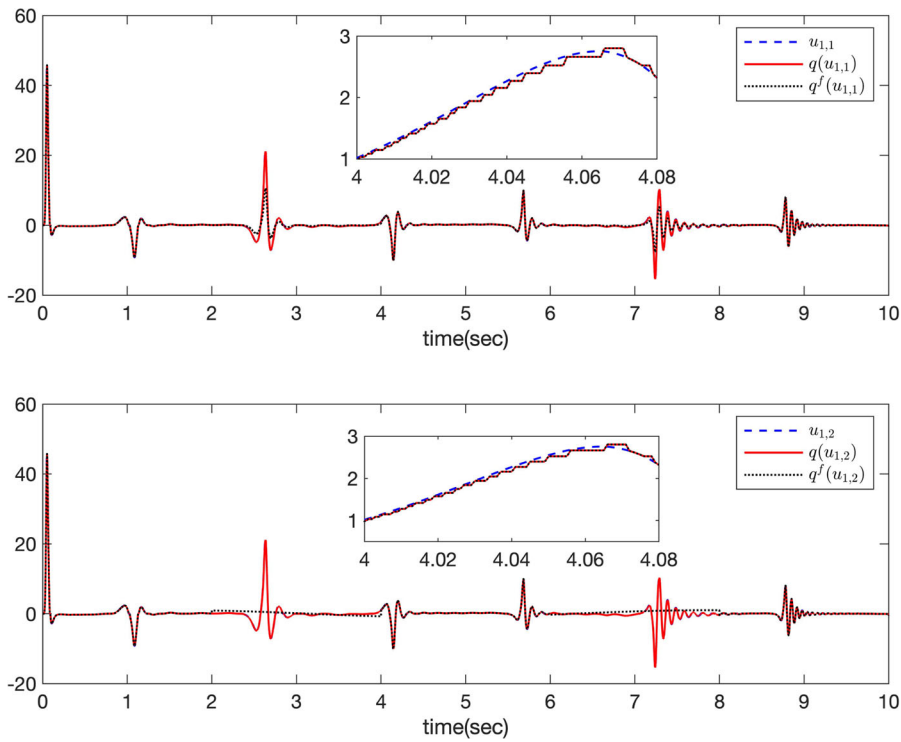


Fig. 9 The trajectories of $u_{1,1}, u_{1,2}, q_{1,1}, q_{1,2}, q^f(u_{1,1}), q^f(u_{1,2})$

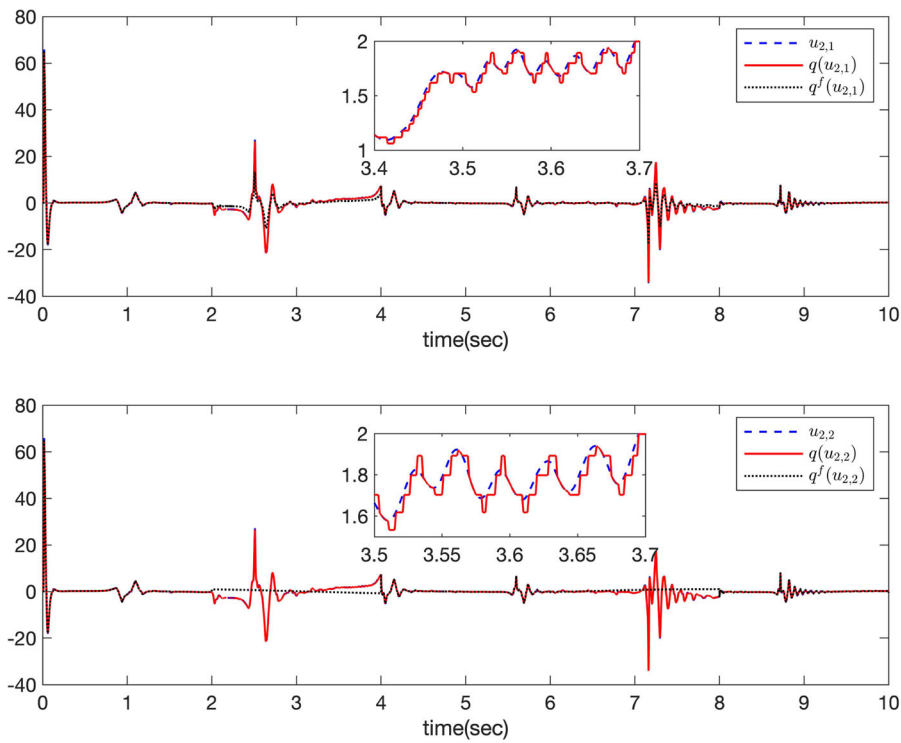


Fig. 10 The trajectories of $u_{2,1}, u_{2,2}, q_{2,1}, q_{2,2}, q^f(u_{2,1}), q^f(u_{2,2})$

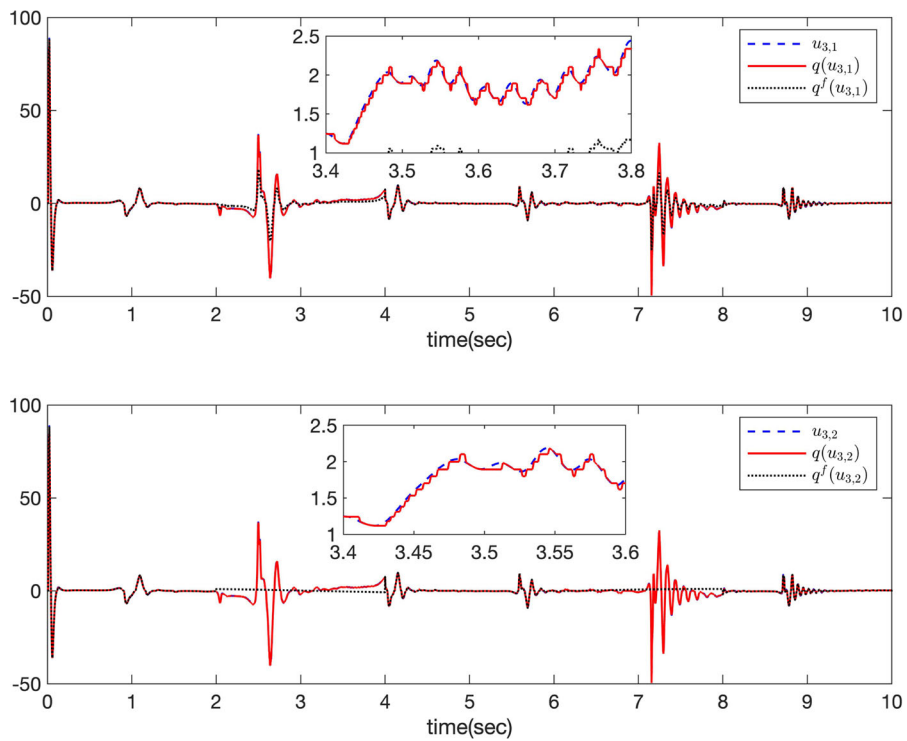


Fig. 11 The trajectories of $u_{3,1}$, $u_{3,2}$, $q_{3,1}$, $q_{3,2}$, $q^f(u_{3,1})$, $q^f(u_{3,2})$

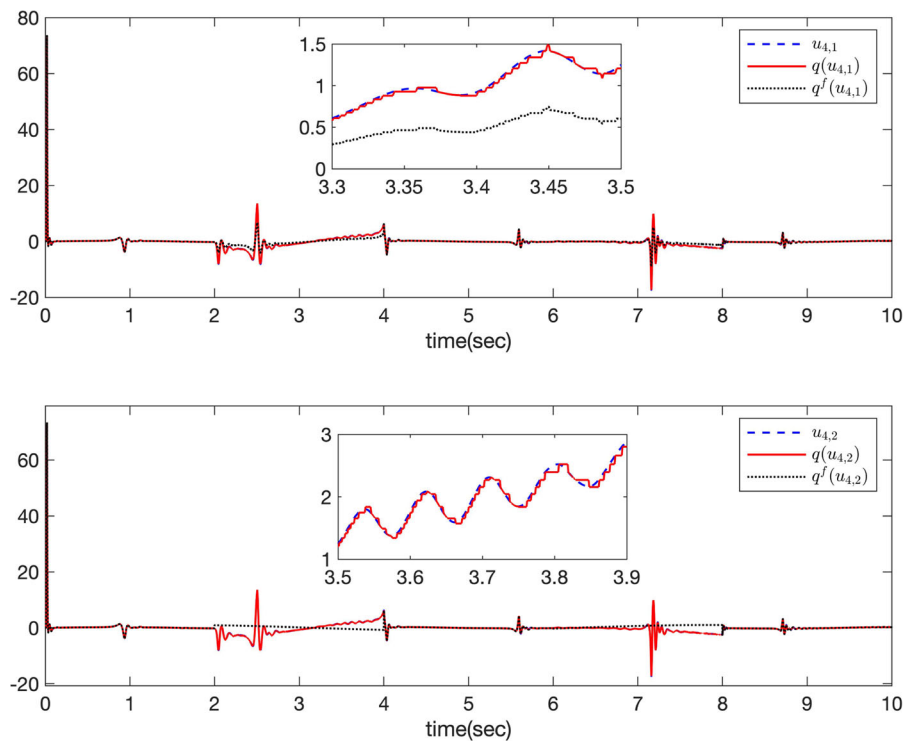


Fig. 12 The trajectories of $u_{4,1}$, $u_{4,2}$, $q_{4,1}$, $q_{4,2}$, $q^f(u_{4,1})$, $q^f(u_{4,2})$

upper bounds of the quantization parameters and actuator fault parameters. Furthermore, the controller constructed within the framework of the backstepping method achieves both the convergence of the tracking errors within a predefined-time frame to a small range and the boundedness of all signals in the closed-loop system. Finally, two simulation examples are provided to demonstrate the effectiveness of the proposed control approach.

Author contributions Li-Ting Lu: formal analysis; methodology; software; writing-original draft. Shan-Liang Zhu: supervision; writing-review and editing. Dong-Mei Wang: writing-original draft. Yu-Qun Han: Funding acquisition; supervision; writing-review and editing. All authors reviewed the manuscript.

Funding This work was supported by the Shandong Provincial Natural Science Foundation, China (No. ZR2020QF055).

Data availability Data sharing is not applicable to this article as no datasets were generated or analysed during the current study.

Declarations

Conflict of interest The authors declares that he has no conflict of interest.

References

- Liang, D., Dong, Y.: Robust cooperative output regulation of linear uncertain multi-agent systems by distributed event-triggered dynamic feedback control. *Neurocomputing* **483**, 1–9 (2022)
- Su, S., Wang, X.K., Tang, T., Wang, G., Cao, Y.: Energy-efficient operation by cooperative control among trains: a multi-agent reinforcement learning approach. *Control Eng. Pract.* **116**, 104901 (2021)
- Xie, K.D., Jiang, Y., Yu, X., Lan, W.Y.: Data-driven cooperative optimal output regulation for linear discrete-time multi-agent systems by online distributed adaptive internal model approach. *Sci. China Inf. Sci.* **66**(7), 1–16 (2023)
- Su, H.S., Wang, X.F., Yang, W.: Flocking in multi-agent systems with multiple virtual leaders. *Asian J. Control* **10**(2), 238–245 (2008)
- Gao, S., Wen, G.G., Zhai, X.Q., Zheng, P.: Finite-/fixed-time bipartite consensus for first-order multi-agent systems via impulsive control. *Appl. Math. Comput.* **442**, 127740 (2023)
- Ni, J.K., Liu, L., Tang, Y., Liu, C.X.: Predefined-time consensus tracking of second-order multiagent systems. *IEEE Trans. Syst. Man Cybern. Syst.* **51**(4), 2550–2560 (2021)
- Ni, J.K., Wen, C.Y., Zhao, Y.: Fixed-time leader-follower quantized output consensus of high-order multi-agent systems over digraph. *Inf. Sci.* **587**, 408–434 (2022)
- Wang, C.L., Wen, C.Y., Guo, L.: Adaptive consensus control for nonlinear multiagent systems with unknown control directions and time-varying actuator faults. *IEEE Trans. Autom. Control* **66**(9), 4222–4229 (2021)
- Wu, W., Tong, S.C.: Fuzzy adaptive consensus control for nonlinear multiagent systems with intermittent actuator faults. *IEEE Trans. Cybern.* **53**(5), 2969–2979 (2023)
- Mao, B., Wu, X.Q., Lü, J.H., Chen, G.R.: Predefined-time bounded consensus of multiagent systems with unknown nonlinearity via distributed adaptive fuzzy control. *IEEE Trans. Cybern.* **53**(4), 2622–2635 (2023)
- Yang, T.T., Dong, J.X.: Practically predefined-time leader-following funnel control for nonlinear multi-agent systems with fuzzy dead-zone. *IEEE Trans. Autom. Sci. Eng.* (2023). <https://doi.org/10.1109/TASE.2023.3289445>
- Li, Y., Wang, C.L., Cai, X., Li, L., Wang, G.: Neural-network-based distributed adaptive asymptotically consensus tracking control for nonlinear multiagent systems with input quantization and actuator faults. *Neurocomputing* **349**, 64–76 (2019)
- Yao, D.J., Dou, C.X., Yue, D., Zhao, N., Zhang, T.: Adaptive neural network consensus tracking control for uncertain multi-agent systems with predefined accuracy. *Nonlinear Dyn.* **101**, 2249–2262 (2020)
- Hao, R.L., Wang, H.B., Zheng, W.: Adaptive neural time-varying full-state constraints quantized consensus control for nonlinear multiagent networks systems without feasibility conditions. *Neural Comput. Appl.* **35**(22), 16457–16472 (2023)
- Wang, M.X., Zhu, S.L., Liu, S.M., Du, Y., Han, Y.Q.: Design of adaptive finite-time fault-tolerant controller for stochastic nonlinear systems with multiple faults. *IEEE Trans. Autom. Sci. Eng.* **20**(4), 2492–2502 (2023)
- Han, Y.Q.: Adaptive tracking control of a class of nonlinear systems with unknown dead-zone output: a multi-dimensional Taylor network (MTN)-based approach. *Int. J. Control* **94**(11), 3161–3170 (2021)
- Lu, L.T., Han, Y.Q., Wang, D.M., Zhu, S.L., Zhou, Q.H.: Adaptive tracking control for a class of nonlinear systems with intermittent actuator faults under prescribe output tracking performance. *Asian J. Control* (2024). <https://doi.org/10.1002/asjc.3317>
- Han, Y.Q.: Design of decentralized adaptive control approach for large-scale nonlinear systems subjected to input delays under prescribed performance. *Nonlinear Dyn.* **106**(1), 565–582 (2021)
- He, W.J., Zhu, S.L., Li, N., Han, Y.Q.: Adaptive finite-time control for switched nonlinear systems subject to multiple objective constraints via multi-dimensional Taylor network approach. *ISA Trans.* **136**, 323–333 (2023)
- Dong, G.W., Li, H.Y., Ma, H., Lu, R.Q.: Finite-time consensus tracking neural network FTC of multi-agent systems. *IEEE Trans. Neural Netw. Learn. Syst.* **32**(2), 653–662 (2021)
- Li, Y.M., Qu, F.Y., Tong, S.C.: Observer-based fuzzy adaptive finite-time containment control of nonlinear multiagent systems with input delay. *IEEE Trans. Cybern.* **51**(1), 126–137 (2021)
- Polyakov, A.: Nonlinear feedback design for fixed-time stabilization of linear control systems. *IEEE Trans. Autom. Control* **57**(8), 2106–2110 (2012)
- Ni, J.K., Liu, L., Liu, C.X., Hu, X.Y., Li, S.L.: Fast fixed-time nonsingular terminal sliding mode control and its appli-

- cation to chaos suppression in power system. *IEEE Trans. Circuits Syst. II Express Briefs* **64**(2), 151–155 (2017)
24. Yang, Y.N., Hua, C.C., Li, J.P., Guan, X.P.: Fixed-time coordination control for bilateral telerobotics system with asymmetric time-varying delays. *J. Intell. Robot. Syst.* **86**, 447–466 (2017)
 25. Sánchez-Torres, J.D., Gómez-Gutiérrez, D., López, E., Loukianov, A.G.: A class of predefined-time stable dynamical systems. *IMA J. Math. Control Inf.* **35**, 1–29 (2018)
 26. Wang, Q., Cao, J.D., Liu, H.: Adaptive fuzzy control of nonlinear systems with predefined time and accuracy. *IEEE Trans. Fuzzy Syst.* **30**(12), 5152–5165 (2022)
 27. Ni, J.K., Shi, P.: Global predefined time and accuracy adaptive neural network control for uncertain strict-feedback systems with output constraint and dead zone. *IEEE Trans. Syst Man Cybern. Syst.* **51**(12), 7903–7918 (2021)
 28. Zhang, T.L., Su, S.F., Wei, W., Yeh, R.H.: Practically predefined-time adaptive fuzzy tracking control for nonlinear stochastic systems. *IEEE Trans. Cybern.* **53**(12), 8000–8012 (2023)
 29. Wang, H.Q., Tong, M., Zhao, X.D., Niu, B., Yang, M.: Predefined-time adaptive neural tracking control of switched nonlinear systems. *IEEE Trans. Cybern.* **53**(10), 6538–6548 (2023)
 30. Shen, D., Xu, Y.: Iterative learning control for discrete-time stochastic systems with quantized information. *IEEE/CAA J. Autom. Sin.* **3**(1), 59–67 (2016)
 31. Yang, Z.C., Hong, Y.G.: Stabilization of impulsive hybrid systems using quantized input and output feedback. *Asian J. Control* **14**(3), 679–692 (2012)
 32. Wu, C.Y., Zhao, X.D.: Quantized dynamic output feedback control and l_2 -gain analysis for networked control systems: a hybrid approach. *IEEE Trans. Netw. Sci. Eng.* **8**(1), 575–587 (2021)
 33. Li, Y.X., Yang, G.H.: Adaptive asymptotic tracking control of uncertain nonlinear systems with input quantization and actuator faults. *Automatica* **72**, 177–185 (2016)
 34. Zhou, J., Wen, C.Y., Yang, G.H.: Adaptive backstepping stabilization of nonlinear uncertain systems with quantized input signal. *IEEE Trans. Autom. Control* **59**(2), 460–464 (2014)
 35. Liu, Z., Wang, F., Zhang, Y., Chen, C.P.: Fuzzy adaptive quantized control for a class of stochastic nonlinear uncertain systems. *IEEE Trans. Cybern.* **46**(2), 524–534 (2016)
 36. Wang, C.L., Wen, C.Y., Lin, Y.: Decentralized adaptive backstepping control for a class of interconnected nonlinear systems with unknown actuator failures. *J. Frankl. Inst.* **352**(3), 835–850 (2015)
 37. Sun, W., Wu, J., Su, S.F., Zhao, X.D.: Neural network-based fixed-time tracking control for input-quantized nonlinear systems with actuator faults. *IEEE Trans. Neural Netw. Learn. Syst.* **35**(3), 3978–3988 (2024)
 38. Wang, J.H., Liu, J.R., Li, Y.H., Chen, C.P., Liu, Z., Li, F.Y.: Prescribed time fuzzy adaptive consensus control for multiagent systems with dead-zone input and sensor faults. *IEEE Trans. Autom. Sci. Eng.* (2023). <https://doi.org/10.1109/TASE.2023.3291716>
 39. Lin, Z.B., Liu, Z., Su, C.Y., Wang, Y.N., Chen, C.L.P., Zhang, Y.: Adaptive fuzzy prescribed performance output-feedback cooperative control for uncertain nonlinear multi-agent systems. *IEEE Trans. Fuzzy Syst.* **31**(12), 4459–4470 (2023)
 40. Gao, S.Q., Liu, J.K.: Adaptive neural network vibration control of a flexible aircraft wing system with input signal quantization. *Aerosp. Sci. Technol.* **96**, 105593 (2020)
 41. Sai, H.Y., Xu, Z.B., He, S., Zhang, E.Y., Zhu, L.: Adaptive nonsingular fixed-time sliding mode control for uncertain robotic manipulators under actuator saturation. *ISA Trans.* **123**, 46–60 (2022)
 42. Du, J., Guo, C., Yu, S., Zhao, Y.: Adaptive autopilot design of time-varying uncertain ships with completely unknown control coefficient. *IEEE J. Ocean. Eng.* **32**(2), 346–352 (2007)
 43. Li, Y.M., Li, K.W., Tong, S.C.: An observer-based fuzzy adaptive consensus control method for nonlinear multiagent systems. *IEEE Trans. Fuzzy Syst.* **30**(11), 4667–4678 (2022)
 44. Zhang, L.L., Chen, B., Lin, C., Shang, Y.: Fuzzy adaptive fixed-time consensus tracking control of high-order multiagent systems. *IEEE Trans. Fuzzy Syst.* **30**(2), 567–578 (2022)
 45. Zhang, Y., Chadli, M., Xiang, Z.R.: Predefined-time adaptive fuzzy control for a class of nonlinear systems with output hysteresis. *IEEE Trans. Fuzzy Syst.* **31**(8), 2522–2531 (2023)
 46. Sun, Y.M., Wang, F., Liu, Z., Zhang, Y., Chen, C.P.: Fixed-time fuzzy control for a class of nonlinear systems. *IEEE Trans. Cybern.* **52**(5), 3880–3887 (2022)
 47. Xie, S.Z., Chen, Q.: Adaptive nonsingular predefined-time control for attitude stabilization of rigid spacecrafts. *IEEE Trans. Circuits Syst. II Express Briefs* **69**(1), 189–193 (2022)
 48. Wang, H.Q., Bai, W., Zhao, X.D., Liu, P.X.P.: Finite-time-prescribed performance-based adaptive fuzzy control for strict-feedback nonlinear systems with dynamic uncertainty and actuator faults. *IEEE Trans. Cybern.* **52**(7), 6959–6971 (2022)
 49. Song, S., Park, J.H., Zhang, B.Y., Song, X.N.: Observer-based adaptive hybrid fuzzy resilient control for fractional-order nonlinear systems with time-varying delays and actuator failures. *IEEE Trans. Fuzzy Syst.* **29**(3), 471–485 (2021)
 50. Wang, W., Wen, C.Y.: Adaptive compensation for infinite number of actuator failures or faults. *Automatica* **47**(10), 2197–2210 (2011)

Publisher's Note Springer Nature remains neutral with regard to jurisdictional claims in published maps and institutional affiliations.

Springer Nature or its licensor (e.g. a society or other partner) holds exclusive rights to this article under a publishing agreement with the author(s) or other rightsholder(s); author self-archiving of the accepted manuscript version of this article is solely governed by the terms of such publishing agreement and applicable law.